

# MODELLING OF A HOVERING QUADCOPTER



AALBORG UNIVERSITY

STUDENT REPORT

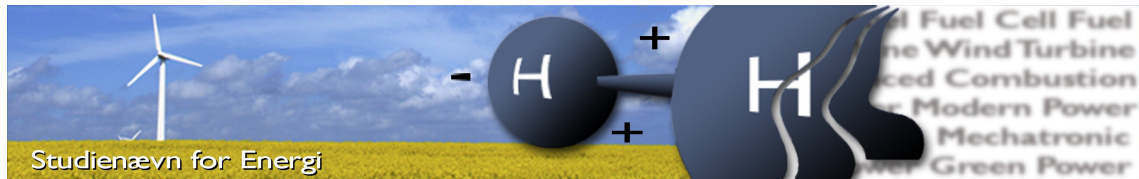
17-12-2014

BY

DANIEL BRUSEN NIELSEN  
TEKLU T.M. TVERMOSE  
KIRSTEN ARNOLDSEN JUHL

RASMUS LYKKE LOMHOLT  
MITCHELL MATEOS AMEZ





**Title:** Modelling of a hovering quadcopter  
**Semester:** 3. semester  
**Semester topic:** Modelling and analysis of simple electrical and thermal systems  
**Project period:** 02.09.14 to 17.12.14  
**ECTS:** 15  
**Adviser:** Peter Omand Rasmussen  
**Project group:** EN-301

#### SYNOPSIS:

The purpose of this project is to derive a mathematical model, which calculates the hover time of a quadcopter. The mathematical model is based on basic theory regarding working principles of a motor, mainly focused on a BLDC motor and the main components of quadcopter. Furthermore, the model can produce motor and propeller characteristics for the quadcopter. In this project the motor of type *Turnigy Multistar 1704 1900 Kv*, propeller of type *GWS EP 7035*, and battery of type *Lipo Receiver Pack 2200 mAh* are used for modelling. The quadcopter with an estimated total mass of 328 g is calculated to have a hover time of approximately 21 minutes. In addition, the mathematical model is able to calculate hover time of a multicopter with a desired number of motors/propellers. The efficiency of the motor is highest at approximately 991 rad/s but the optimal operating point for the load is found at 671 rad/s. Thus, the motor is not operating with the highest efficiency at the optimal operating point.

---

Daniel BRUSEN NIELSEN

---

Kirsten ARNOLDSEN JUHL

---

Rasmus LYKKE LOMHOLT

---

Teklu T. M. TVERMOSE

---

Mitchell UHRSKOV MATEOS AMEZ

Printings: 3  
Number of pages: 90  
Appendix: 5, CD attached

**By signing this document every member of the group confirms that they have contributed equally to the project work and each group member is collectively responsible for the content of the student report. Besides every group member is responsible that the report contains no plagiarism.**

# Nomenclature

## Symbols

Symbol	Term	Units
$F$	Force	N
$V$	Volume	$\text{m}^3$
$v$	Velocity	$\text{m}/\text{s}$
$E$	Energy	J
$P$	Power	W
$B$	Magnetic field	T
$C$	Capacity	Ah
$I$	Current	A
$U$	Voltage	V
$\varepsilon$	Electromotive force	V
$R$	Resistance	$\Omega$
$m$	Mass	kg
$A$	Area	$\text{m}^2$
$T$	Temperature	K, $^{\circ}\text{C}$
$p$	Pressure	Pa
$l, w, r, y, h$	Length, width, radius, height, thickness	m
$\eta$	Efficiency	Dimensionless
$\rho$	Density	$\text{kg}/\text{m}^3$
$\dot{m}$	Mass flow	$\text{kg}/\text{s}$
$t$	Time	s
$\tau$	Torque	Nm
$J$	Moment of inertia	$\text{kg}\cdot\text{m}^2$
$\omega$	Angular velocity	rad/s

## Acronyms

Acronyms	Description
<i>DC</i>	Direct Current
<i>EMF</i>	Electromotive Force
<i>CEMF</i>	Counter Electromotive Force
<i>BDC</i>	Brushed DC
<i>BLDC</i>	Brushless DC
<i>AOA</i>	Angle of Attack
<i>RAF</i>	Relative Air Flow
<i>ESC</i>	Electronic Speed Controller
<i>GPS</i>	Global Positioning System
<i>CPU</i>	Central Processing Unit
<i>RC</i>	Radio Controlled
<i>KVL</i>	Kirchhoff's Voltage Law
<i>RPM</i>	Revolutions Per Minute
<i>IMU</i>	Inertial Measurement Unit

## Constants

Constants	Description	Unit
<i>g</i>	Gravitational acceleration	9,82 m/s <sup>2</sup>
<i>K<sub>φ</sub></i>	Torque sensitivity constant/ CEMF constant	Nm/A, Vs
<i>K<sub>l</sub></i>	Lift/Torque constant	J/N
<i>K<sub>t</sub></i>	Propeller constant	Nm/N
<i>C<sub>d</sub></i>	Drag coefficient	Dimensionless
<i>Re</i>	Reynolds number	Dimensionless

# Preface

Aalborg Universitet 17.12.2014

This report has been completed by third semester students at the Energy program at Aalborg University. The overall theme of the project is modeling and analyzing of energy technology systems. The report is written from 02.09.2014 - 17.12.2014.

## Reading guide

Through the report the *Harvard method of references* will be used. The text is referenced to a source with [Surname, Year]. Sources with an unknown year are stated as [Surname, Unknown]. If an author is used several times, it will be given a letters such as [Surname, Year a], and an edited figure will be referenced as '[Surname, Year] ed.'

In the bibliography, a date for when the source was last used, will be given. All Internet sources are included on a CD. The enclosed CD will also contain all relevant data and scripts from the project.

Furthermore, first time an abbreviation is used, the word is fully written followed by the abbreviation in parentheses. Formulas, figures, etc. are numbered according to the chapter in which they are used. For instance, the first figure in Chapter 2 will be numbered figure 2.1, etc.



# Contents

<b>Nomenclature</b>	<b>iii</b>
Symbols . . . . .	iii
Acronyms . . . . .	iv
Constants . . . . .	iv
<b>Preface</b>	<b>v</b>
<b>1 Introduction</b>	<b>1</b>
1.1 Quadcopters . . . . .	1
1.2 Initial problem . . . . .	1
<b>2 Problem analysis</b>	<b>3</b>
2.1 Hovering . . . . .	3
2.2 Components of a quadcopter . . . . .	7
2.3 Black box . . . . .	7
2.4 Possibilities . . . . .	8
<b>3 Problem statement</b>	<b>9</b>
<b>4 Components of a quadcopter</b>	<b>11</b>
4.1 Battery . . . . .	11
4.2 BLDC motors . . . . .	13
4.3 Aerodynamics regarding the propeller of a quadcopter . . . . .	24
4.4 Recap of main components . . . . .	29
4.5 Black box components . . . . .	30
<b>5 Characteristics of a motor and propeller system</b>	<b>33</b>
5.1 Hardware . . . . .	33
5.2 Hover time of a quadcopter . . . . .	34
5.3 Determination of the power losses of the system . . . . .	40
5.4 Efficiency of the system . . . . .	45
<b>6 Evaluation</b>	<b>47</b>
6.1 Data sets . . . . .	47
6.2 Varying numbers of motors/propellers . . . . .	50
6.3 Efficiency vs. power output . . . . .	50
<b>7 Conclusion</b>	<b>51</b>
<b>8 Perspective</b>	<b>53</b>
8.1 Operating point . . . . .	53
8.2 The blade element theory . . . . .	53

8.3 Torque speed relation . . . . .	53
<b>Bibliography</b>	<b>57</b>
<b>Appendices</b>	<b>61</b>
<b>Appendix I - Experiment-equipment</b>	<b>63</b>
<b>Appendix II - Lift and power experiment</b>	<b>67</b>
<b>Appendix III - Mechanical losses - experiment</b>	<b>71</b>
<b>Appendix IV - Matlab scripts</b>	<b>73</b>
<b>Appendix V - Modification of the discharge time equation</b>	<b>79</b>

# 1 | Introduction

An *Unmanned Ariel Vehicle* (UAV) is an aircraft that can fly autonomously or can be controlled from the ground. [Villasenor, 2012]. There are many types of UAV's for different kinds of assignments, e.g. military, surveillance, firefighting etc. UAV's are also becoming popular in the commercial sector where they are used for a wide area of assignments [Lyle, 2010].

## 1.1 Quadcopters

A quadcopter is a type of UAV. The prefix of 'quadcopter' is caused by the fact that it has two sets of two identical propellers - thereby a total of four propellers. On each propeller there is a motor attached which generates angular momentum on the propeller. One set of propellers rotates clockwise the other set counterclockwise. Quadcopters vary in sizes and weights depending on their purpose. Some companies have even tried to incorporate quadcopters in their delivery methods. Other use them for aerial photography and surveillance.



Figure 1.1: Different kinds of quadcopters with their speciality, (a)[Griffiths, 2013], (b)[Finkbuilt, 2014] .

## 1.2 Initial problem

The usage of quadcopters is increasing [Dussault, 2014]. It is important that the quadcopter can fulfill its purpose, e.g. when using a quadcopter for surveillance it is essential that the quadcopter does not have a short time of flight. The expectations of the hover time need to be met [Dussault, 2014].

**It is desired to know the hover time, which is why this project main focus is on modeling a quadcopter simulation, which calculates the hover time.**

This project subject has been outlined by *UASworks*. The main focus of this project is to calculate the hover time of the quadcopter for a certain choice of main components. Through an email-correspondence with a contact member of *UASworks*, *Henrik Gade* limitations regarding weight and efficiency of the quadcopter are set:

*"Lift with a maximum efficiency and a limit of the efficiency with maximum 50 -100 gram, and the double at full speed for a motor. We expect that it weighs 200-400 grams"* (translated).

It is on behalf of these assumptions made by *UASworks* that the quadcopter will be modeled.

## 2 | Problem analysis

The purpose of the problem analysis is to clarify possibilities for calculating the hover time. A quadcopter consists of various components, which will be described through the following chapters. Subsequently appropriate factors regarding the hover time will be outlined. This chapter is mainly based on the book *Essential University Physics*[Wolfson, 2011]. and aims to explore ways to resolve the initial problem which will result in a problem statement.

### 2.1 Hovering

The simplest form of quadcopter flying is hovering, where conditions like ground effect, wind etc. are not accounted for. It is important to understand the concept of hovering. It is maintaining a constant height above the ground. Hence, both acceleration and velocity of the quadcopter is zero [Watkinson, 2003].

#### 2.1.1 Acting forces

Thrust is a force, which enables the quadcopter to hover. It is used to overcome the weight of the system (the gravitational force).

Figure 2.1 shows a 2-dimensional representation of the acting forces. The upward pointing arrow ( $F_t$ ) shows the lift and the downward pointing arrow ( $F_g$ ) represent the gravitational force.

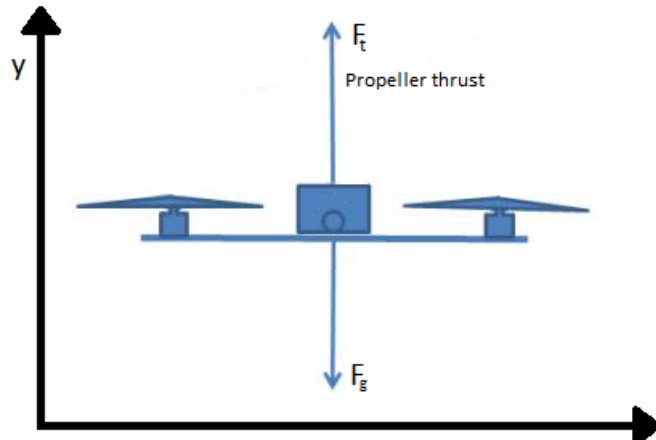


Figure 2.1: A 2-dimensional representation of the acting forces.

## Downward force

The weight is an important factor when considering the hover time of a quadcopter. When hovering the only acting forces are the gravitational pull and the counter acting thrust generated. The gravitational force is given by in equation 2.1.

$$F_g = m_Q \cdot g \quad (2.1)$$

Where  $m_Q$  is the mass of the quadcopter and  $g$  the is gravitational acceleration. In order for the quadcopter to hover, the upward force (thrust) must equal the gravitational pull, as in equation 2.2.

$$F_g = F_t \Leftrightarrow 0 = F_g - F_t \quad (2.2)$$

## Upward force

The quadcopter propels air downwards to produce lift. The propellers accelerate the airstream in a negative  $y$  direction (downwards) and the counteracting force produced is the thrust which is shown at figure 2.2.

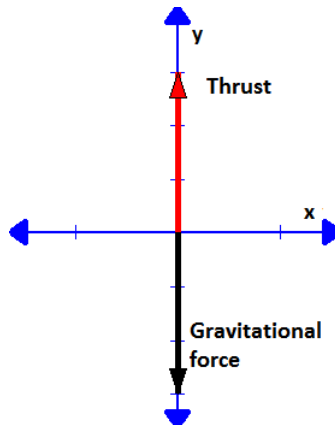


Figure 2.2: A 2-dimensional representation of the counteracting forces that produce thrust.

Due to *Newton's third law* the force, which the quadcopter exerts on the air,  $F_{air}$  equals the force, which the air exerts on the quadcopter  $F_t$  - just in the opposite direction. The force, the air stream exerts on the quadcopter, is expressed in equation 2.3.

$$-F_{air} = F_t = \frac{d(m_{air} \cdot v_{air})}{dt} \quad (2.3)$$

The time differential  $dt$  can be described as the time it takes an infinitesimal mass of air,  $dm_{air}$  to reach a infinitesimal vertical distance,  $dy$ , at a given velocity  $v_{air}$ . The velocity is given by equation 2.4.

$$v_{air} = \frac{dy}{dt} \Leftrightarrow dt = \frac{dy}{v_{air}} \quad (2.4)$$

Inserting equation 2.4 into 2.3 it becomes:

$$F_t = \frac{d(m_{air} \cdot v_{air}^2)}{dy} \quad (2.5)$$

If  $dV_{air}$  is a volume differential of the air and  $\rho_{air}$  the air density, the mass of the air  $dm_{air}$  can be found by equation 2.6.

$$dm_{air} = \rho_{air} \cdot dV_{air} \quad (2.6)$$

The shape of the airstream can be described as infinitely many cylinders placed down through the airstream. The volume of an air cylinder with a mass  $dm_{air}$  is then a volume differential  $dV$  consisting of the cross-sectional area of the airstream,  $A$ , and the height,  $dy$

$$dV_{air} = dy \cdot A \quad (2.7)$$

As seen by figure 2.3 the radius of the cylinder of air increases with the vertical distance downwards,  $y$ , from the propellers.

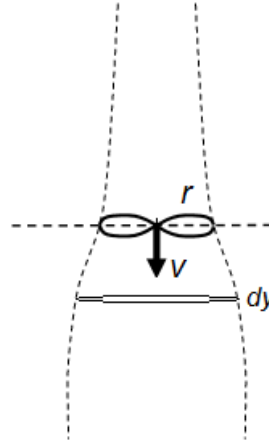


Figure 2.3: A 2-dimensional simplified representation of the generated airstream [Intech] ed.

The cross-sectional area,  $A$ , of a cylinder is given as  $\pi r^2$ , where  $r$  is the radius. Substituting  $\pi r^2$  and equation 2.6 into equation 2.5, it yields:

$$F_t = \frac{\rho_{air} \pi r^2 dy \cdot v_{air}^2}{dy} = \rho_{air} \pi r^2 v_{air}^2 \quad (2.8)$$

The radius,  $r$ , and the velocity of the airstream are variables of the chosen motor and propeller. It appears that they are proportional to the exerted forces. This means that an increase of any of these variables increases the exerted thrust force. The density ( $\rho$ ) of the air varies due to the temperature (the warmer the air, the less dense it is). The density of the air can not be controlled, thus it is set to be a constant factor.

## Hover condition

The upward force (thrust) must equal the gravitational pull  $F_g$  (shown in equation 2.2) in order for the quadcopter to hover.

By substituting equation 2.8 and 2.1 into 2.2, it is possible to find the connection between the main factors. It yields:

$$m_Q \cdot g = \rho_{air} \pi \cdot (r \cdot v_{air})^2 \Leftrightarrow \sqrt{\frac{g}{\rho_{air} \cdot \pi}} = \frac{r \cdot v_{air}}{\sqrt{m_Q}} \quad (2.9)$$

Due to the fact that  $g$ ,  $\rho_{air}$ , and  $\pi$  are constants, the left side of equation 2.9 is substituted with  $k$ , which simplifies to:

$$k = \frac{r \cdot v_{air}}{\sqrt{m_Q}}, \quad \text{or as} \quad m_Q \cdot k^2 = (r \cdot v_{air})^2 \quad (2.10)$$

Thus, by equation 2.10 it appears that the product of the radius (or lenght) of the propellers and the velocity of the airstream are inverse proportional. The square of both are proportional to the mass of the quadcopter [Wolfson, 2011].

### 2.1.2 Factors which affect the operation of the quadcopter

In order to hover the gravitational force needs to be canceled out. Therefore the total weight of the system is an important factor. Modifications on other components will generally have an impact on the total mass. The thrust is generated by an interaction between the propellers and the motors. Externally the weather can also be a significant limitation since air densities vary with different kinds of weather. The variables can be summarized as followed:

- The weight of the system.
- Aerodynamic, mechanical, and electrical effects.
- The current delivered from the battery.
- The rotational torque delivered from the motors.
- The amount of thrust generated by the propellers.
- The weather conditions during flight.

These variables are dependent of one another and have to be set correctly, in order for the quadcopter to operate at the optimal rate. However, they are not necessarily proportional to one another. Though changing just one factor will not linearly change the hover time [Gade, 2014], [Dussault, 2014].

## 2.2 Components of a quadcopter

A quadcopter consists of several different components which includes:

1. The motor
2. The propeller
3. The battery
4. The frame
5. Internal components: GPS, CPU, and IMU
6. Electronic speed controller (ESC)

The components is shown on figure 2.4.



Figure 2.4: Components of a quadcopter [Garage, 2014] ed.

As described earlier the quadcopter consist of four motors with four propellers attached. The battery functions as the energy source and delivers power to the motors. The motors converts the electrical power into a rotational momentum. The frame consists of four arms with a motor attached at each and a center to contain the battery. The ESC regulates the voltage drop across the motor and the current input to the motor. An IMU, a CPU, and an RC receiver is equipped and is crucial for controlling the quadcopter.

## 2.3 Black box

The focus of this project is on the energy converting devices. Therefore a black box will be used to take the losses into account. A black box is a device, which ignores the internal mechanisms of a system or components and focuses solely on the output in response to the input. The black box is situated between the energy producing component of the system (the battery) and the energy consuming components of the system (motor and propeller). The black box consumes energy and has an additional mass. The following components are included in the black box and are given estimated values.

The components in the black box outlined in figure 2.5 is:

- The accelerometer
- Internal components like GPS, CPU, etc.

- Radiocontrol
- The frame
- The ESC
- Mountable components such as cameras, etc.

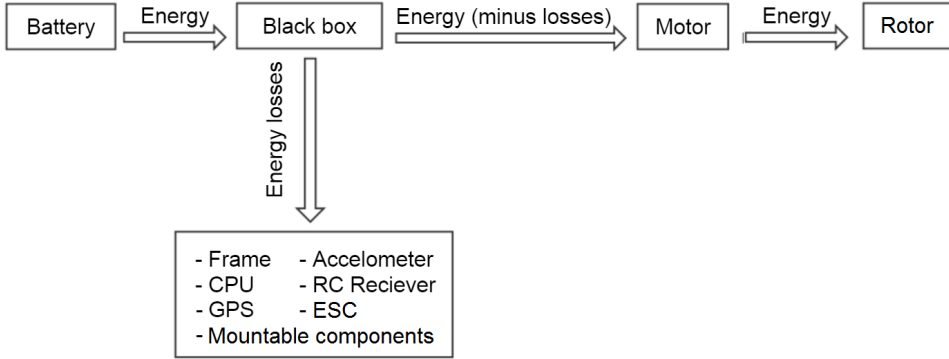


Figure 2.5: A simple overview of electrical energy losses in the black box, where the components of the black box are outlined.

## 2.4 Possibilities

The power source delivers power to the system. This electrical power input is converted into mechanical power in the motor which drives the propeller. Hence thrust is generated. With this in mind, there are several factors, which affects the hover time:

- The length of the propellers.
- The angular velocity of the propellers.
- The weight.
- The capacity of the battery.
- The efficiency of the motor.

When operating these factors are fixed. Thus, the quantity of each has to balance in best possible way with one another.

### 2.4.1 Focus

It is desired to model a quadcopter in *MatLab*, where it is possible to regulate the quantities of the previously mentioned components. Hence, the motors, propellers, and the battery will be considered, while the components in the black box will be given a fixed value. It is possible to base the model, so it arises from any of the above factors. However, it can be argued that the system highly depends on the motors and the propellers. The motors draw a certain amount of current from the battery. The angular velocity of the propellers is limited from the amount of mechanical energy delivered from the motors. Both of which depend on the size of the motors. Thus, the primary focus of this project lies on the motors. This means that the description and modeling regarding the motors throughout this project will be more detailed.

## 3 | Problem statement

The main topic of this project is to create a mathematical model that can calculate the hover time of the quadcopter by inserting a combination of motor, propeller, and battery constants. The quadcopter will only be considered operating in steady-state, which means it is not maneuverable. In this case 'maneuverable' is the ability to accelerate (set-off) and decelerate (land), and the ability to pitch (turn). To achieve this, the key aspects and components of the quadcopter will be further described. The project will focus on producing a mathematical model in which a motor and propeller set-up can be characterized. Here the hover time, power losses and efficiency of the set-up be calculated.

### **How would a hover time for a quadcopter with a certain motors/propeller set-up be calculated via a mathematical model, when the model is mainly focused on the motor?**

The problem can be outlined in smaller issues, which will also be described through this report.

- Which forces apply to the system?
- How do the motor and the propeller work together?
- Is it possible to calculate the hover time for a motor/propeller set-up through experimental data, and how?
- How would the efficiency of the system be calculated?
- Is it possible to develop a mathematical model to describe the quadcopters characteristics and how would this model be designed?



# 4 | Components of a quadcopter

In this chapter the main components of the quadcopter will be outlined. The main components are the battery, the motor, and the propeller. The physics regarding the motor, the electronic components, and the aerodynamic design will be described. Finally the content of the black box will be outlined along with its effect on the system.

## 4.1 Battery

The battery provides power to the system. When discharging, it converts stored chemical energy into electrical energy. A battery is basically a source of electromotive force (EMF or  $\varepsilon$ ) with an internal resistor,  $R_{int}$ , connected to a load, as shown in figure 4.1.

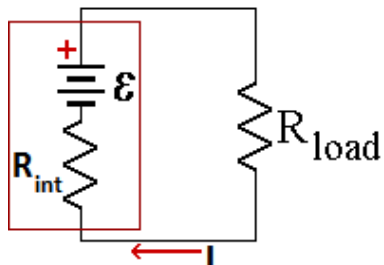


Figure 4.1: A diagram of a battery connected to a load [Raymond A. Serway, 2010b] ed.

The EMF of a battery is the maximum possible voltage it can provide between the terminals, whereas the internal resistance is due to the chemical losses and the natural resistance of the wires material (an idealized battery has no internal resistance, hence the terminal voltage equals the EMF). The EMF is given by the sum of the voltage drop over the internal resistance and the load resistance, which is outlined in equation 4.1.

$$\varepsilon = IR_{int} + IR_L \quad (4.1)$$

The voltage drop across the resistor  $R_L$  is not the EMF due to the internal resistance, but  $IR_L$ . So rearranging equation 4.1, it yields the voltage across the terminals ( $U_{terminal}$ ) of the battery.

$$U_{terminal} = \varepsilon - IR_{int} \quad (4.2)$$

Isolating equation 4.1 for the current,  $I$ , it yields:

$$I = \frac{\varepsilon}{R_{int} + R_L} \quad (4.3)$$

From equation 4.3 it can be seen that the current and the resistances,  $R_L$  and  $R_{int}$ , are inverse proportional, which means that an increased internal resistance, reduce the delivered current. When a battery is used as a power source to a quadcopter with a low internal resistance. This results in a higher power transfer to the system. The power transfer will be further described later on in this chapter.

#### 4.1.1 Discharge

When a load, which in this case is the components of the quadcopter, is connected to the battery, current starts to flow through the circuit. Hence, the battery is discharging at a certain rate. When looking at a battery with a constant discharging rate the discharging time is also the hover time of the quadcopter. The capacity of the battery refers to the amount of electrical charge it is able to deliver at the rated voltage. The power the battery is able to deliver is expressed by 4.

$$P_{battery} = U_{terminal} \cdot I_{battery} \quad (4.4)$$

$I$  is the current drawn from the battery, and  $U_{terminal}$  is the voltage drop across the terminals of the battery.

The energy stored in a battery is expressed by equation 4.5.

$$E_{battery} = C \cdot U_{terminal} \quad (4.5)$$

$C$  is the capacity of the battery. At a given operation point of the quadcopter, the quadcopter draws a specific approximately constant amount of current (steady state). Inserting equation 4.5 in 4, an expression for the discharge time of the battery can be found.

$$P_{battery} = \frac{E_{battery}}{C} \cdot I_{battery} \quad (4.6)$$

By multiplying equation 4.6 with a quantity, time,  $t$ , 4.6 yields 4.7.

$$t = \frac{C}{I_{battery}} \quad (4.7)$$

From equation 4.7, the greater current drawn, the shorter time of discharge. The discharge time is related to the hover time of the quadcopter [Mikael Cugnet, 2010]. An increase of the battery capacity will result in an increase of the mass of the battery, if the energy density is constant. Energy density,  $E_{dens}$ , is a quantity, which describes stored energy per unit mass. In relation to a battery this is basically a measure for the chemical energy stored,  $E_{total}$ , in relation to its mass,  $m_{battery}$ , see equation 4.8.

$$E_{dens} = \frac{E_{total}}{m_{battery}} \quad (4.8)$$

A modified version of equation 4.7 (Peukert's law) is outlined in *Appendix V - Modification of the discharge time equation*.

## Power transfer

Power transfer is a quantity, which describes the amount of power delivered from the battery to the circuit. *The maximum power transfer theorem* states that, in order to obtain maximum external power from a source with a finite internal resistance, the resistance of the load must equal the resistance of the source as viewed from its output terminals. Thus, to determine the maximum power output, the internal resistances and the load resistance equal each other. The internal resistant is a fixed property of the battery, thus it can not be regulated. Whether it is a efficient power source depends on the specifications of the battery.

## Efficiency

The efficiency of the battery can be expressed by 4.9

$$\eta = \frac{P_{out}}{P_{out} + P_{loss}} \Rightarrow \frac{R_L}{R_L + R_{int}} \quad (4.9)$$

By equation 4.9, it appears that if the internal resistances converges towards zero, the efficiency approaches 100 %. When  $R_{int}$  and  $R_L$  equals one another, the power output is at its maximum, but by equation 4.9 it appears that the efficiency is 50 %.

## 4.2 BLDC motors

A DC motor is basically a rotating coil between two magnetic poles. The poles generate a magnetic field. When a current is flowing through the coil, the field exerts a force on the coil. The force is given by the magnitude of the current,  $I$ , and the cross product of the length vector,  $\vec{l}$ , of the coil and the magnetic field,  $\vec{B}$ , as shown in equation 4.10.

$$\vec{F} = I \cdot \vec{l} \times \vec{B} \quad (4.10)$$

The force direction of equation 4.10 is illustrated by figure 4.2.

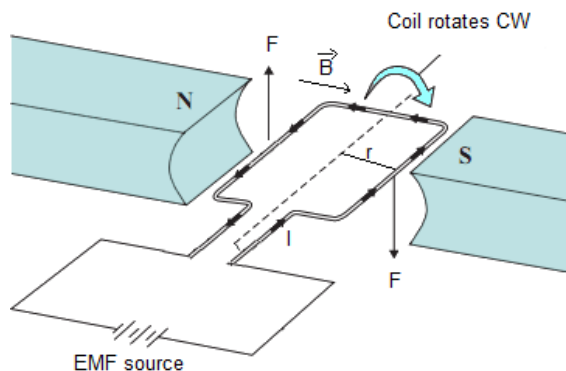


Figure 4.2: The force the magnetic field exerts on the coil [MatLab] ed.

When rotating, the motor produces torque. Torque is in essence the tendency of a force to rotate an object about an axis. Torque can be thought of as a twist to an object, which

is given by the product of the force,  $F$ , expressed by equation 4.10 and the radius of the coil,  $r$ . Equation 4.11 expresses it explicit.

$$\vec{\tau} = \vec{r} \times \vec{F} \quad (4.11)$$

There are two common types of DC motors, the BLDC (Brushless DC) motor and the BDC (Brushed DC) motor. The most common drawbacks of a BDC motor are the need of a commutator, and the use of brushes, which wear and tear over time. In the BLDC motor the functions of the commutator and brushes are implemented by electronics components, which require no maintenance. Some of the advantages are outlined below:

- Longer operation life
- Greater angular velocity
- Noiseless operation
- Higher dynamic response
- High efficiency

The BLDC motor is basically a synchronous electric motor, which means that the rotation of the shaft is synchronized with the frequency of the current supplied. In the desired system of this project, a BLDC motor will be implemented. In the following section the main source used is the paper *Brushless DC Motors* by A. Karadimov.

#### 4.2.1 Structures

BLDC motors can be constructed in several physical configurations.

##### Inrunner and outrunner configuration

An *inrunner* configuration means that the permanent magnets are part of the rotor, where three stator windings surround the rotor. An *outrunner* or external-rotor configuration, the stator coils form the centre of the motor, while the permanent magnets spin within a rotor which surrounds the core [Eric Wahl, 2014].

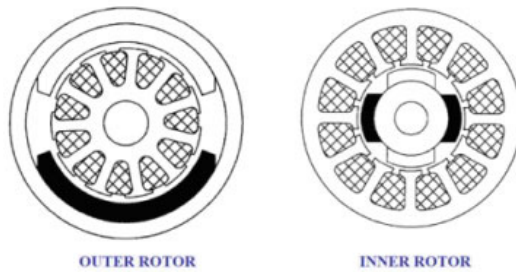


Figure 4.3: The difference between an inrunner and outrunner motor [Corporation, 2011].

##### Wye-, delta configurations

There are two common configurations in order to connect the windings - the wye- and delta configuration, shown by figure 4.4.

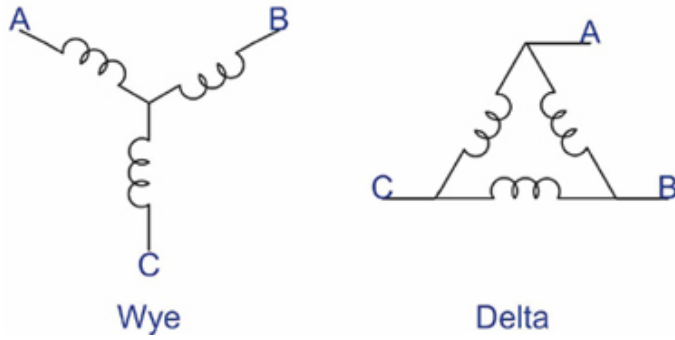


Figure 4.4: Schematic for a wye and delta configuration [Embedded, 2014]

The delta configuration connects three coils to each other in series circuit. The wye configuration connects the coils in a single point, with gives a parallel circuit.

The delta configuration generates less torque at low speed, but is able to gain higher maximum velocity than the wye configuration, whereas the wye configuration generates higher torque at low velocity, but is not able to gain as high velocity. However, the wye configuration is usually the most efficient, due to the design of the circuits. The delta configuration is a series circuit, which means only half voltage is applied across the coils, in relation to the wye configuration, which increases the resistive losses. Thus, the wye configuration is the most used in a BLDC motor [Eric Wahl, 2014].

## Phases

The most efficient and common BLDC motor is three phased. Figure 4.5 shows the induced EMF in the coils as a function of the angular position [Microchip, 2003].

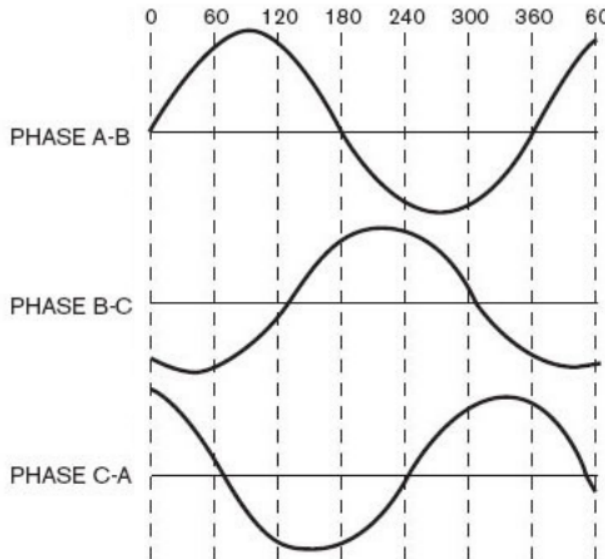


Figure 4.5: The sinusoidal voltage of a three phased motor. [Microchip, 2003].

As shown on figure 4.5, the phases are displaced by 120 degrees, which allows a smoother output. Figure 4.6 shows a diagram of a three phased BLDC motor.

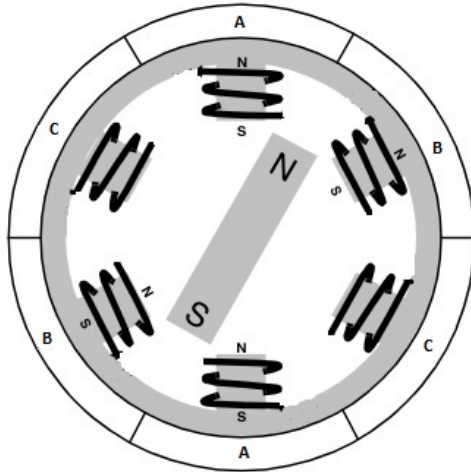


Figure 4.6: A diagram of a three phased motor [BLDC wikidot] ed.

The current through the respective coils, corresponds to the phases (A, B, and C) shown in figure 4.5 and depends on the displacement of the magnet in figure 4.6.

#### 4.2.2 Commutation

The BLDC motor requires a method to detect the position of the rotor (or the magnetic poles) to switch the currents of the coils, which drives the motor. This detecting device is either a Hall element (magnetic sensor, see figure 4.7) or an optical sensor (phototransistor). A BLDC motor with three phases has six states of commutation.

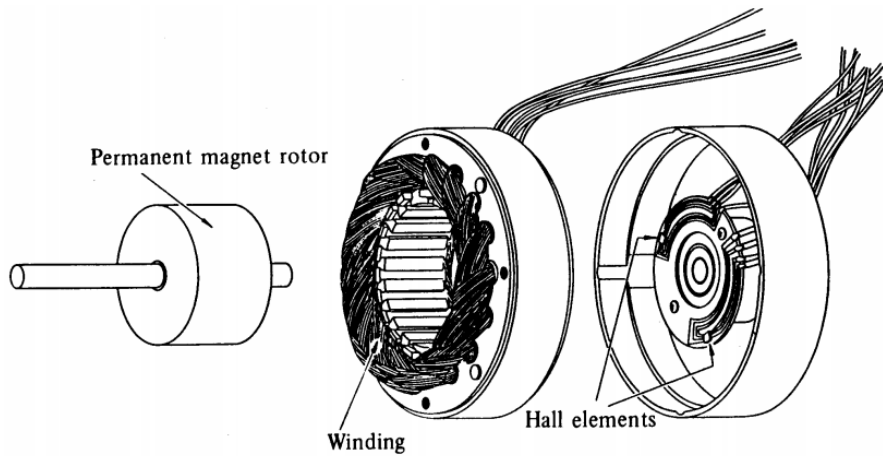


Figure 4.7: The motor structure of a three-phase BLDC motor [Karadimov, 2000].

#### Bipolar BLDC motor

A BLDC motor can have different phases. The most commonly used is a three-phase BLDC motor. A BLDC motor with different number of three phases will not be described in this project, because they require a more complex combination of transistors or are unsymmetrical.

A BLDC motor can be unipolar and bipolar. In a unipolar motor only one coil can be activated at a time and it can only have an identical pole (north or south). In a bipolar motor multiple coils can be activated at the same time and consist of both poles (north and south).

Both consist of a controller, a number of coils and a set of permanent magnets. A controller is required to activate the right coils at the right time. The activation of the coils are controlled by transistors and a sensor attached to the shaft. The sensor can in this case be a phototransistor linked with different transistors. On figure 4.8 a phototransistor is illustrated.

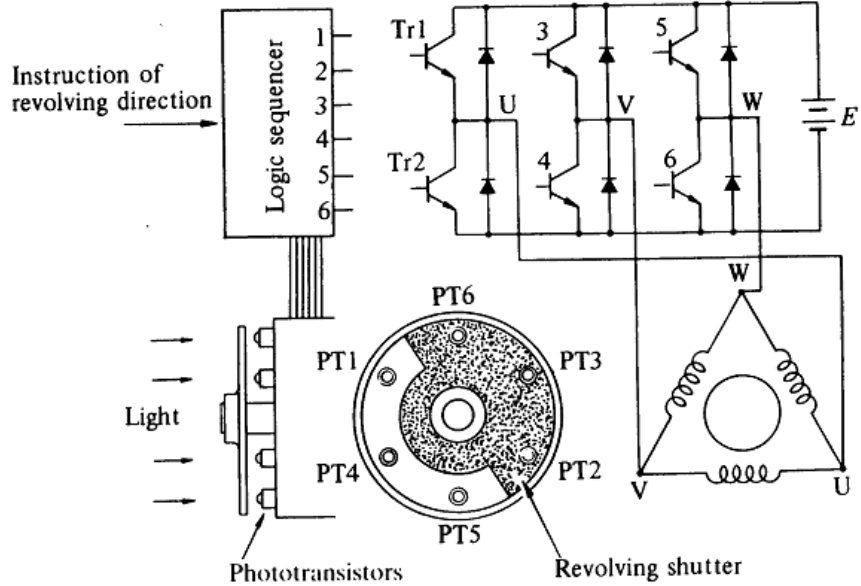


Figure 4.8: A photo-sensitive bipolar-driven six pole BLDC motor. PT<sub>x</sub> is phototransistor number x, Tr<sub>x</sub> circuit transistor number x. U, V, W are voltages [Karadimov, 2000].

When phototransistors are exposed to light their corresponding coils will be energized and the shaded ones will deenergize their coils. When a coil activates it attracts a permanent magnet so the shutter will rotate and the phototransistors shift. Hence, a new signal is transmitted. When the coils are continuously activated the BLDC motor will rotate. If the shifts between the coils are failing or out of order, the motor will stall. Therefore, the synchronization between the phototransistors and the coils is important.

A bipolar type of motor is most commonly used, because it is more efficient, as the currents flow through multiple coils.

The principle of a three-phased bipolar circuit with optical detecting will be described. As shown on figure 4.8 there are six phototransistors, PT<sub>1</sub>, PT<sub>2</sub>, PT<sub>3</sub>, etc. They are separated equally by 60 degrees. The phototransistors will activate the coils when detecting light. In order to make the motor operate continuously, a special circuit is required. This circuit involves a logic sequencer and a bridge circuit, which switches the currents in the right order, see figure 4.8.

By figure 4.9, it appears that current will flow through the transistors; Tr<sub>1</sub>, Tr<sub>4</sub>, and Tr<sub>5</sub>. The solid arrows indicate the directions of the magnetic fields, which is generated by the current in each phase. The blue arrow indicates the total magnetic field within the stator.

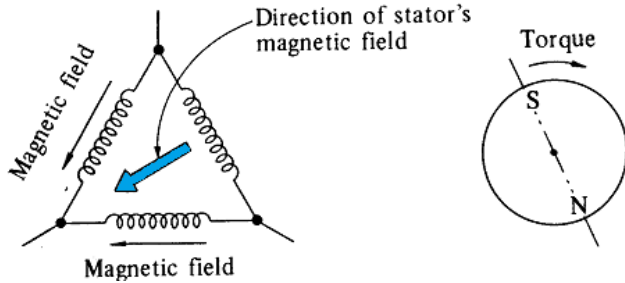


Figure 4.9: Stator field due to the currents through coils illustrated to the left, generated torque at rotor due to the influenced rotor field illustrated to the right [Karadimov, 2000] ed.

As shown by figure 4.9 the rotor is placed such that its field flux forms an angle of 90 degrees with respect to the magnetic field of the stator. Due to this magnetic field a clockwise torque is generated on the rotor. By a turn of 30 degrees the rotor position makes PT5 switch off and PT6 switch on, seen by figure 4.8. At this point, the north pole of stator turns 60 degrees clockwise, and the south pole of the rotor will be attracted by it. The stator pole will continue to revolve as soon as the pole of the rotor is approaching. This creates a continuous clockwise rotation. A full overview of the sequence and the rotation of the transistor is illustrated by figure 4.10.

ON-OFF sequence	1	2	3	4	5	6
Tr 1	1	1	1	0	0	0
2	0	0	0	1	1	1
3	0	0	1	1	1	0
4	1	1	0	0	0	1
5	1	0	0	0	1	1
6	0	1	1	1	0	0

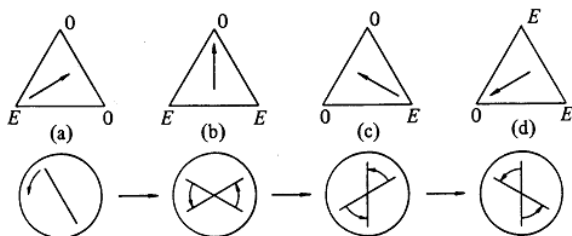


Figure 4.10: An overview of on/off-values of the transistors in a sequence. 1 means ON, 0 means OFF [Karadimov, 2000] ed.

It is possible to reverse the rotational direction of the rotor by rearranging the logic sequencer in a way so light-exposed phototransistors switch off the current in their corresponding coils. Contrary to the previous circuit this makes the shaded phototransistors imply a current running through their corresponding coils. The resultant ON-OFF sequence for the transistors shown on figure 4.11 will then have the exact opposite values. Hence, the revolutions will be counter-clockwise.

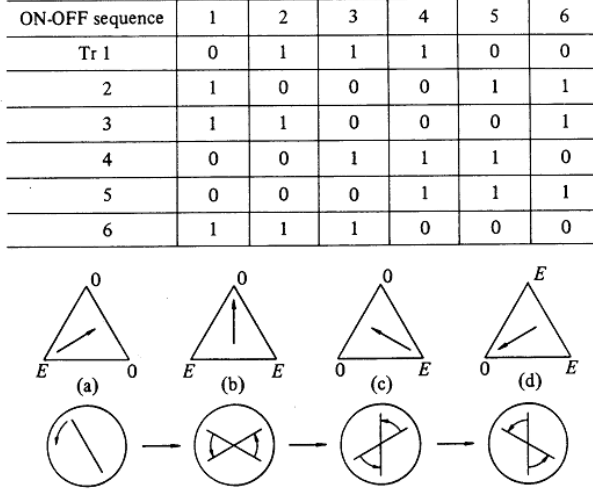


Figure 4.11: An overview for the inverted sequence of that in figure 4.10 [Karadimov, 2000] ed.

#### 4.2.3 Self-induced electromotive force

The electromotive force (EMF) is a voltage generated by the coils when the motor is in an operating state. The principle of self-induced EMF originates from *Faraday's law of electromagnetic induction*. It states that when a conductor is placed in a changing electromagnetic field,  $\frac{d\Phi_B}{dt}$ , an electric field,  $\vec{E}$ , is produced. This is the case in a DC motor.

$$\oint \vec{E} d\vec{r} = -\frac{d\Phi_B}{dt} \quad (\text{Faraday's law}) \quad (4.12)$$

The EMF ( $\varepsilon$ ) for any closed path can be expressed as the line integral of  $\vec{E} d\vec{r}$  (the left side of equation 4.12). By *Lenz' Law* the induced EMF opposes the voltage drop apply to the coils. This is called a counter EMF (CEMF or  $\varepsilon_{counter}$ ) because the induced EMF opposes the voltage across the motor and reduces the total voltage across the terminals.

The CEMF can be expressed by equation 4.13.

$$\varepsilon_{counter} = \omega \cdot K_\varphi \quad (4.13)$$

Equation 4.13 shows that the induced CEMF and angular velocity of the motor are proportional.  $K_\varphi$  is the proportionality coefficient (CEMF constant). It can be described as the product of voltage and time.

As the coil begins to rotate, the induced CEMF opposes the applied voltage. Hence, the overall voltage drop across the terminals of the motor decreases.

#### 4.2.4 The electromechanical torque of the motor

The electromechanical torque produced by a motor can be expressed by:

$$\tau_{em} = I_{motor} \cdot K_\varphi \quad (4.14)$$

Equation 4.14 shows that the internal motor current is proportional to the electromechanical torque produced.  $K_\varphi$  is the coefficient of proportional (torque sensitivity). Despite being equal to the CEMF constant, in equation 4.14 it represents the torque produced for every ampere of current drawn by the motor [Raymond A. Serway, 2010b].

## Mechanical losses

When the motor is operating, power losses, due to mechanical factors, occurs. Figure 4.12 shows the torques which act on the motors during operation.

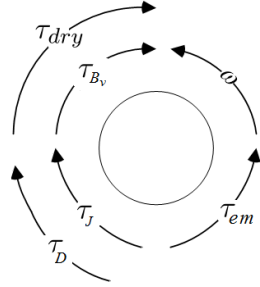


Figure 4.12: Torque affecting the operation of the motor. The arrows represent the twist due to the torque (the length of the arrows do not represent the magnitude of the torque) .

The twist of the electromechanical torque has the same direction as the angular velocity, as seen in figure 4.12. The quantities  $\tau_J$ ,  $\tau_{B_v}$ , and  $\tau_{dry}$  oppose the torque  $\tau$ . Thus, the electromechanical torque is given by equation 4.15.

$$\tau_{em} = \tau_J + \tau_{B_v} + \tau_D + \tau_{dry} \quad (4.15)$$

Torque due to the produced drag  $\tau_D$  depends on the specific propeller. The drag torque can be described as the product of the radius,  $r$ , and the drag force,  $F_D$ , which will be described in section *Aerodynamics regarding the propeller of a quadcopter*:

$$\tau_D = F_D \cdot r = B\omega^2 \quad (4.16)$$

The torque due to the moment of inertia,  $\tau_J$ , of the coil is given by equation 4.17.

$$\tau_J = J \cdot \frac{d\omega}{dt} \quad (4.17)$$

As shown by equation 4.17  $\tau_J$  is only sufficient, when the rotating coil is accelerating (starting up) or deceleration (stopping), otherwise the change of the angular velocity,  $\frac{d\omega}{dt}$  will be zero. Hence,  $\tau_J$  is zero when operating in steady state.

The moment of inertia of the propeller,  $J$ , with thickness,  $h$ , can be described as a flat plane with area ( $l \times w$ ) about a perpendicular axis, expressed by equation 4.18 [Cengal A. Yunus, 2012].

$$J = \frac{1}{12} m_i \cdot (l^2 + w^2) \quad (4.18)$$

Here  $m_i$  is the mass of the flat plan,  $l$  is length of the propeller and  $w$  is the average width. The mass of the propeller can then be calculated by equation 5.15.

$$m_i = \rho \cdot h \cdot l \cdot w \quad (4.19)$$

The dry friction,  $\tau_{dry}$ , is the torque required to overcome the static friction, when the motor begins operating, therefore  $\tau_{dry}$  is zero when working in steady state.

The loss due to material friction (losses of the bearings) is given by the product of the viscosity of the material of interest,  $B_v$ , and the angular velocity,  $\omega$ . It is shown explicit by equation 4.20.

$$\tau_{B_v} = B_v \cdot \omega \quad (4.20)$$

Hence, the electromechanical moment,  $\tau_{em}$ , can be expressed by equation 4.21.

$$\tau_{em} = B\omega^2 + B_v\omega + \tau_{dry} + J \cdot \frac{d\omega}{dt} \quad (4.21)$$

Thus, the electromechanical torque can be expressed by the sum of the torque due to the moment of inertia,  $\tau_J$ , the torque due to the drag force,  $\tau_{B_v}$ , the torque due to the iron losses and friction in the bearings,  $\tau_D$ , and the torque required to overcome the static friction,  $\tau_{dry}$ . There are two operating states of the motor, where one of the part in equation 4.21 becomes zero - cut-off mode and steady state:

When cut-off the electro mechanical torque,  $\tau_e$ , will become zero, and equation 4.15 becomes:

$$0 = \tau_{B_v} + \tau_B + \tau_{dry} + \tau_J \quad (4.22)$$

When operating in steady state, the torque due to the inertia, will become zero, and equation 4.15 becomes:

$$\tau_{em} = \tau_{B_v} + \tau_B + \tau_{dry} \quad (4.23)$$

#### 4.2.5 Equivalent Circuit

The voltage across the terminals of the motor is the sum of the voltage drop of each component (the internal resistance  $R_a$ , the inductor  $L_a$ , and the self-induced EMF  $\varepsilon$ ), shown by figure 4.13.

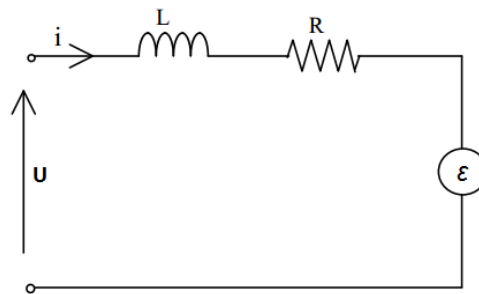


Figure 4.13: Circuit diagram over an electric DC motor [Karadimov, 2000] ed.

Using *Kirchhoff's Voltage Law* (KVL), equation 4.24 expresses the total voltage drop across the terminals of the motor.

$$U_{terminal} = R_{motor} \cdot I_{motor} + L_{motor} \cdot \frac{dI}{dt} + K_\varphi \cdot \omega \quad (4.24)$$

If the system is not accelerating, the current is in steady state, and not changing over time, thus  $\frac{dI}{dt}$  becomes zero. This is also the case when the quadcopters is hovering. Hence, the voltage drop across the inductor becomes zero. Thus, equation 4.24 reduces to:

$$U_{\text{terminal}} = R_{\text{motor}} \cdot I_{\text{motor}} + K_\varphi \cdot \omega \quad (\text{Steady state}) \quad (4.25)$$

The product of  $K_\varphi \omega$  is the CEMF ( $\varepsilon_{\text{counter}}$ ), and the product of  $IR_{\text{motor}}$  is the voltage drop due to the resistance in the windings. Depending on how fast the motor spins, CEMF is generated, which reduces the current running through the motor, which reduces the overall loss in the circuit [Bright Hub Engineering, 2011], [Raymond A. Serway, 2010b].

The phase equivalent circuit of a BLDC motor is shown below in figure 4.14. If assumed that the voltage across the terminals,  $U$  and CEMF,  $\varepsilon$ , are sinusoidal and have a frequency  $\omega$  the equivalent circuit can be expressed as on fig 4.14b. The values  $U$ ,  $I$ , and  $\varepsilon$  from the figure are *rms* values and phasors. If the circuit is in steady state the circuit equation yields (from KVL):

$$U_{\text{terminal}} = \varepsilon + (R_{\text{motor}} + j\omega L)I_{\text{motor}} \quad (4.26)$$

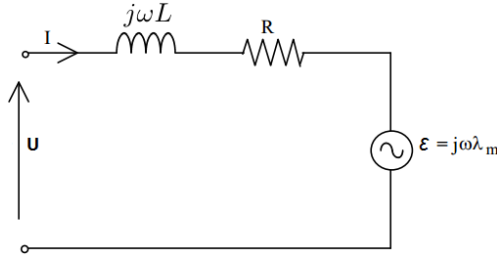


Figure 4.14: The figures show (a) the dynamic per phase circuit of a BLDC motor (b) the same circuit in steady state [Karadimov, 2000] ed.

### Efficiency of the motor

The efficiency is defined as the required output devided by the input.

$$\eta = \frac{P_{\text{out}}}{P_{\text{in}}} \quad (4.27)$$

The input power is given by eqaution 4.28

$$P_{\text{in}} = U \cdot I \quad (4.28)$$

The power output describes the mechanical energy, the motor is able to deliver over a period of time. It is given by equation 4.29.

$$P_{\text{out}} = P_{\text{in}} - P_{\text{loss}} = \tau \cdot \omega - (P_{\text{mec}} + P_{\Omega}) \quad (4.29)$$

$P_{\text{mec}}$  is the mechanical losses, as explained in subsection *Mechanical losses* (the motor is assumed to operate in steady state), and  $I^2R$  is the ohmic losses (the internal losses in the wires). Inserting this in equation 4.27, it yields:

$$\eta = \frac{\tau \cdot \omega}{I \cdot (\varepsilon_{\text{delivered}} - \varepsilon_{\text{counter}}) - (P_{\text{mec}} + I^2 R)} \quad (4.30)$$

By inserting the expressions for torque and angular velocity, given by equation 4.11 and 4.13, it yields:

$$\eta = \frac{I_{motor} \cdot \varepsilon_{counter}}{I_{motor}(\varepsilon_{delivered} - \varepsilon_{counter}) - (P_{mec} + I^2R)} \quad (4.31)$$

As seen by equation 4.31, as the CEMF increases, the efficiency,  $\eta$ , increases as well. Since the CEMF is proportional to the angular velocity, the efficiency increases as the angular velocity increases. In addition, if the torque increases, the motor slows down, which causes the CEMF to decrease. This reduction in the CEMF increases the current in the coils, thereby increases the power needed from the battery. For this reason, the power requirements for running a motor are greater for heavy loads than for light ones. If the motor is allowed to run under no mechanical load, the CEMF reduces the current to a value just large enough to overcome energy losses due to internal resistant and friction. If a load blocks the motor, the lack of a CEMF can lead to high current in the internal wires of the motor. High current can lead to a break down [Bright Hub Engineering, 2011], [Raymond A. Serway, 2010b].

## 4.3 Aerodynamics regarding the propeller of a quadcopter

A quadcopter consists of a number of propellers that create lift when rotating. The design of the propeller blades is an important factor.

A quadcopter-propeller with aerodynamic design have the ability to create a lift force [Cengal A. Yunus, 2012]. The lift makes it possible for the quadcopter to hover. This requires the magnitude of lift,  $F_t$ , to equal the magnitude of gravitational pull,  $F_g$ :

$$F_t = F_g \quad (4.32)$$

In the following sections it will be described how the aerodynamic design of a propeller can cause lift. This type of structure is called an aerofoil or airfoil, see figure 4.15.

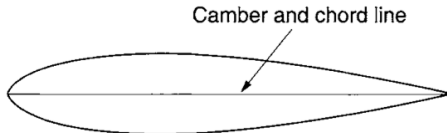


Figure 4.15: A typical design of an aerofoil [Watkinson, 2003].

### 4.3.1 The concept of lift

The Swiss scientist *Daniel Bernoulli* discovered that a flow of air moving over a surface forms a lower pressure. This is called *the Venturi effect*. The greater the velocity difference of the airflow at the bottom and top side of the propeller, the greater the pressure differences, and the bigger the lift. In this subsection, it will be described how the velocity difference is created [Cengal A. Yunus, 2012].

A surface with an aerodynamic design is a surface that interacts with the airflow. A propeller has an aerodynamic design with a changing cross-sectional area in which the air flows. The airflow is illustrated as streamlines in figure 4.16. When the air flow in the cross-sectional area decreases, the streamlines are forced closer to each other. This results in an increase of the velocity of the airflow in order to preserve the mass flow. The air that passes on the bottom side of the aerofoil is slowed down because of the aerodynamic design. The air that passes on the top side of the aerofoil will then be compressed due to the aerodynamic design so that the velocity increases as in figure 4.16.

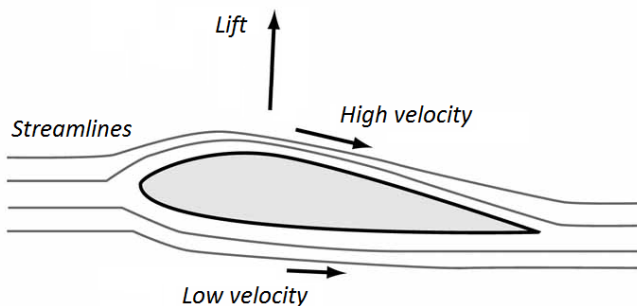


Figure 4.16: An aerodynamic design in an airflow. When the streamlines of the airflow is compressed, there is an increase of the velocity of the airflow to preserve the mass flow [Wetzel, 2012] ed.

The compression results in an increase of the velocity of the airflow, which results in a lower pressure. The pressure difference between the two sides (the top- and bottom side) leads to lift [Cengal A. Yunus, 2012].

The velocity difference of the airflow can be described through a venturi-tube, see figure 4.17.

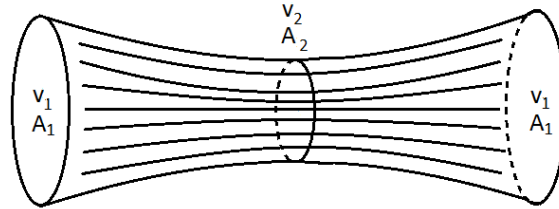


Figure 4.17: An airflow through a venturi-tube with a narrowing in the middle.

A venturi-tube is a cylindrical tube in which there is a narrowing in the middle. When a flow of air is passing through the pipe there will be a change in velocity,  $v$ , and a change in the cross-sectional area,  $A$ . Because there is only change in the velocity and cross-sectional area, it is possible to present following:

$$\dot{m} = A_1 \cdot v_1 \cdot \rho_{air} = A_2 \cdot v_2 \cdot \rho_{air} \Leftrightarrow A_1 \cdot v_1 = A_2 \cdot v_2 \quad (4.33)$$

This means that an aerofoil's ability to create a lift can be derived from the velocity change that occur, when the wind passes a different cross-sectional area [Cengal A. Yunus, 2012].

#### 4.3.2 Bernoulli's equation

In this subsection it will be described how a velocity difference can create a pressure difference. Here the relation between the velocity change of the airflow and the created pressure difference (on the top and bottom side of the aerofoil) will be described.

The effect of the airflow on a aerofoil can be derived from a long cylinder tube, see figure 4.18, in which the air flows through with a velocity,  $v$ , in the time  $\Delta t$ .

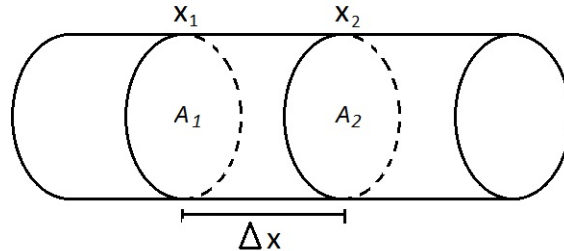


Figure 4.18: A cylinder where a fluid flows through with a given velocity in a given time.

The distance between the two points  $x_1$  and  $x_2$  can be described as following:

$$x_2 - x_1 = \Delta x = v \cdot \Delta t \quad (4.34)$$

The volume is given by:

$$V = \frac{m}{\rho} \quad (4.35)$$

The volume, V, can be described with the distance between the two points,  $\Delta x$  and the cross-sectional area, A. By inserting equation 4.35 and 4.34, it yields:

$$V = \Delta x \cdot A = \frac{m}{\rho} = v \cdot \Delta t \cdot A \quad (4.36)$$

$$m = v \cdot \Delta t \cdot A \cdot \rho \quad (4.37)$$

The kinetic energy of the airflow can be described:

$$E_{kin} = \frac{1}{2} \cdot m \cdot v^2 \quad (4.38)$$

Bernoulli equation for a smooth airflow can then be written as kinetic energy together with the static pressure energy of the airflow (static pressure energy is the random thermal motion of the molecules together with the potential energy):

$$E_{total} = E_{kin} + E_{static} = cst \Rightarrow \frac{E_{total}}{V} = \frac{1}{2} \cdot \rho \cdot v^2 + \rho \cdot g \cdot h + p = cst \quad (4.39)$$

V is the volume,  $\rho$  is the density of the air, v is the air velocity, p is the pressure. The total energy is preserved thereof, the equation is equal to a constant [Cengal A. Yunus, 2012].

I.e. the Bernoulli equation for the smooth airflow can be expressed by the kinetic energy together with the static pressure energy. When the aerofoil is hit by an airflow, it is split into two different airflows (top and bottom side of the aerofoil) with different velocities. The potential energy can be neglected, when looking at the top and bottom side of a small aerofoil. When the total energy of the airflows (top and bottom of the propeller) both are equal, because of the mass conservation, following is possible:

$$\frac{1}{2} \cdot \rho \cdot v_1^2 = \frac{1}{2} \cdot \rho \cdot v_2^2 + \Delta p \quad (4.40)$$

It can be concluded from the equation 4.40 that an air velocity difference between the top and bottom side of the aerofoil can create a pressure difference. As earlier explained this pressure difference,  $\Delta p$ , generates a lift.

### 4.3.3 Acting forces on the aerofoil

Now it is known how a pressure difference can course lift since Bernoulli's equation states that due to a change of the velocity of the airflow a pressure difference is created. This change is utilized by the propellers to generate lift. In this section the movement of the airflow on the propellers will be described together with the lift reaction, which the airflow creates.

The flow created around the propellers is called the relative airflow, RAF, and is illustrated in figure 4.19. RAF can be illustrated as a orthogonal vector which contributes on creating a lift. A propeller only produces a lift if it is slightly inclined on the RAF at an angle, also called the angle of attack, AOA. The AOA is the angle between an original velocity

vector of the airflow and the new velocity vector of the airflow created by the pitch. The AOA is illustrated on figure 4.19.

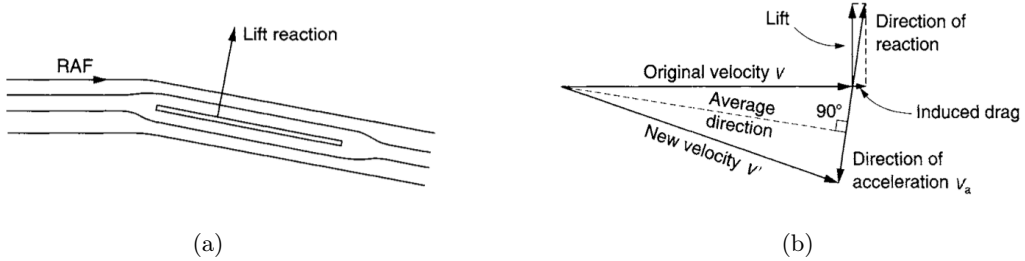


Figure 4.19: The figures show the generated lift from two different points of view (a) Relative air flow[Watkinson, 2003], (b) Angle of attack[Watkinson, 2003] .

The lift is generated when the velocity vector of the airflow changes at an AOA as illustrated in figure 4.19, where  $v$  is the original velocity vector of the airflow and  $v'$  is the velocity vector of the airflow after hitting the propeller. The change of the velocity vector will result in a counter reaction and is represented as a velocity vector  $v_a$  and illustrates the direction of the acceleration of the airflow.

The lift is the vertical force of the counter-reaction. The horizontal force of the counter-reaction is called the drag force.

### The lift force of a propeller

The laminar airflow on the propeller will result in a upward force (thrust). In an ideal motor/propeller system the force,  $F_t$ , generated on the propeller relation between the power,  $P$ , the motor expends can be described by equation 4.41 [Gibiansky, 2012]:

$$P = F_t \cdot \frac{dx}{dt} \Leftrightarrow P = F_t \cdot v_{air} \quad (4.41)$$

Here the power is equal to the generated force (thrust) multiplied by the air velocity. The air velocity is the distance,  $dx$ , the air is forced downwards by the rotating propeller per time unit,  $dt$ .  $v_{air}$  is the velocity of the air when the quadcopter is hovering. The air surrounding the quadcopter is assumed to be have a negligible velocity throughout this project. Furthermore, the air velocity is expressed in equation 4.42 as a function of the thrust, the density of the air, and the area which the propeller spans [Gibiansky, 2012]:

$$v_{air} = \sqrt{\frac{F_t}{2\rho A_s}} \quad (4.42)$$

Combining equation 4.42 and 4.41 yields:

$$P = \sqrt{\frac{F_t^3}{2\rho A_s}} \quad (4.43)$$

The power the motor consumes can also be described as in equation 4.44 [Gibiansky, 2012]:

$$P = \frac{K_\varphi}{K_\varphi} \cdot K_l \cdot F_t \cdot \omega \quad (4.44)$$

Here the  $K_\varphi$ ,  $K_l$ ,  $A_s$ , and the density of the air are constants, so it can be written as a new constant,  $b$ .  $K_\varphi$  is a motor constant derived from the magnetic flux and is given for the specific motor, it describes the CEMF induced per angular velocity.  $K_l$  is a proportionality constant between the lift force,  $F_t$ , and the torque,  $\tau$ , and depends on the measures of the blades.

When combining equation 4.44 and 4.43 and isolating the thrust,  $F_t$ , it yields:

$$F_t = \left( K_l \cdot \sqrt{2\rho A_s} \cdot \omega \right)^2 \Rightarrow F_t = b\omega^2 \quad (4.45)$$

This means that the thrust,  $F_t$ , is proportional to  $\omega$  squared, with  $b$  as the proportionality constant.

Note that equation 4.45 only describes the thrust of one set of motor connected to a propeller. In this project the quadcopter consists of 4 sets of motors and propellers, which means that the thrust of all four sets have to be accounted for. When a quadcopter is hovering the thrust of each propeller must be equal.

## Drag force of a propeller

The drag force can be described as in equation 4.46.

$$F_d = \frac{1}{2}\rho_{air}v_{air}^2AC_d \quad (4.46)$$

$v_{air}$  is the velocity of the RAF.  $A$  is the planform area of the aerofoil.  $\rho_{air}$  is the density of the air and  $C_d$  is the drag coefficient of the propeller. The drag coefficient is a function of *Reynold's number*,  $Re$ .  $C_d$  varies according to the objects position and size, speed, flow direction, fluid viscosity, and fluid density [Cengal A. Yunus, 2012].

A greater AOA will initially generate a greater lift, since the change of velocity vector will be higher. However a higher AOA would result in a greater drag force and would eventually lead to a stall. When a aerofoil is stalling, it can not generate enough lift to overcome the gravitational pull.

The drag force,  $F_D$ , on the propeller generates a drag torque,  $\tau_D$ , as previously mentioned in subsection *Mechanical losses*. Assuming that all of the drag force is applied at the end of the rotor (a distance  $r$  from the rotational axis, also the radius), equation 4.47 applies. This assumption is done to simplify the relation between the drag-torque and the angular velocity.

$$\tau_D = F_D \cdot r \quad (4.47)$$

Inserting equation 4.46 in 4.47, it yields:

$$\tau_D = \frac{1}{2}\rho_{air}v^2AC_d \cdot r \xrightarrow{v=\omega r} \tau_D = \frac{1}{2}\rho_{air}\omega^2r^3AC_d = B\omega^2 \quad (4.48)$$

In this project the drag force will not be theoretically calculated, because it requires a known drag coefficient, which is a function of *Reynold's number*,  $Re$ , which is unknown. Though the drag torque can be found experimentally. This will be further explained in *Characteristics of a motor and propeller system*.

## 4.4 Recap of main components

In the previous section the main components and their physics are described: The battery, the motors, and the propellers.

The battery functions as a power source that provides power to the motor. The magnets within the BLDC motor have a magnetic field. The magnetic flux through the area of the current carrying coil generates a magnetic force. This magnetic force rotates the permanent magnets attached to the rotor and produce a torque, which rotates the propeller, which generates thrust. The thrust is proportional to the angular velocity squared, which makes it possible to find the generated thrust at a specific power input. The generated thrust is then equal the gravitational force when hovering.

The formulas from chapter four regarding the physics of the quadcopter will be used to establish a mathematical model, which simulates a hovering quadcopter.

## 4.5 Black box components

The black box components have already been outlined in section *Black box*. The components in the black box are:

- The frame
- The ESC
- Internal components like GPS, RC receiver, CPU, and IMU
- Mountable components such as cameras, etc.

There are power losses in the internal components, and additional mass which the generated thrust has to overcome in order to hover. The mountable components such as cameras are not taken into account, due to the fact that these are optional attachments. The following section will outline the effects the different components in the black box will have on the hover time of the quadcopter. In this section, arguments for the assumptions are made in relation to a quadcopter with a total mass of maximum 400 g, which means that the black box components are chosen with respect to this mass [Gade, 2014].

### 4.5.1 The frame

The frame does not have any energy consumption, but the additional mass will require a greater thrust from the propellers and therefore it needs to be considered.



Figure 4.20: A quadcopter carbon fibre frame [Pyramid models].

The mass depends on several factors, e.g. how big the quadcopter is supposed to be and which material the frame is made of. A big quadcopter has large propellers and therefore it needs a larger area for the propellers to spin around. For this project it is assumed that the frame is made out of carbon fibre, since it is a very lightweight but compact material.

### 4.5.2 The electrical components

The four motors in a quadcopter each have an ESC that regulates the individual speed of the motor. An ESC has a loss by having internal resistance and has a mass. The mass from an ESC is very small compared to the total mass. It depends on the current

and voltage it needs to deliver. An ESC for a BLDC motor e.g. from the retail store *HobbyKing 10 A ESC 1 A UBEC* can deliver 10 A will weigh about 8 g all included. A higher current means a bigger weight. The power losses from an ESC are due to internal resistance.

The other electrical components in a quadcopter placed in the center consist of many different parts. The most important are the IMU (accelerometer and gyroscope), Microcontroller (CPU) and the radio controlled (RC) receiver.

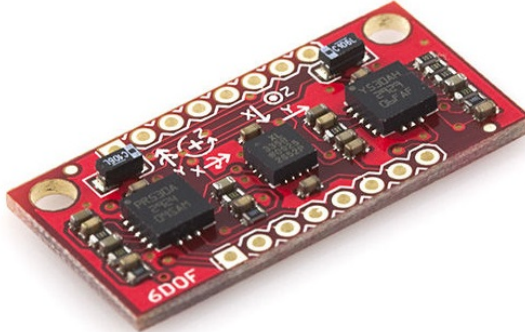


Figure 4.21: An *Arduino* accelerometer module [Lauszus].

The mass of all the internal components are very small compared to the total mass. Receivers usually weighs about 1-10 g depending on how big the quadcopter is. An *Assan R6M* RC receiver, which is a light weight 2,4 GHz, receiver weighs about 4,5 g. CPU and IMU boards are the smallest components in term of weight. Adding up the mass the total mass of the components of the black box will be 50 g [Gade, 2014]

The power losses of the components will draw a current with a certain voltage. By this the total power loss from the black box can be calculated. The components draws 100 mA of total current with a voltage of 4 V, or the same as 0,4 W.

#### 4.5.3 Black box overview

The black box takes the losses between the energy producing components (the battery) and the energy consuming (the motors) into account. The black box gives a general energy consumption (losses), and an additional mass.

The initial overview of the black box is that the power losses from the electronic components are 0,4 W and 50 g, and the frame mass is 90 g.

The values of the additional mass and power losses of the components, in the black box, will be used in the following chapter regarding the mathematical model.



# 5 | Characteristics of a motor and propeller system

This chapter focuses on presenting characteristics of a hovering quadcopter, which can describe values such as the hover time and the efficiency. These characteristics are made by creating *MatLab scripts*, which can calculate certain values and relations like for the quadcopter system. The script will be programmed so the different main components can be changed if wanted, e.g. if a heavier frame is needed to stabilize the quadcopter, the new hover time can be calculated if the frame input is changed. The purpose of the second part of this chapter is to calculate the efficiency of the quadcopter. The focus will lie on the main components of the quadcopter, whereas the components which do not vary with each quadcopter setup like ESC, and the frame is being put in the black box. In figure 5.1 the flow of energy and main components is outlined.

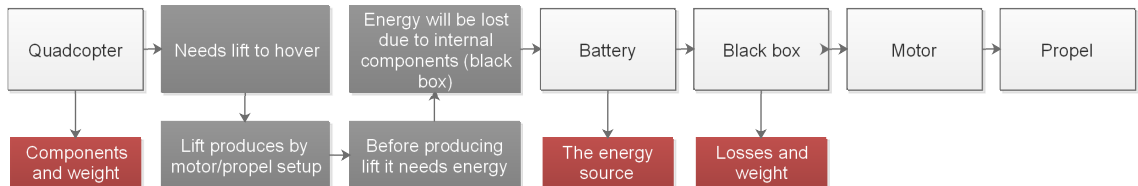


Figure 5.1: Overview of system model

The finished *MatLab script* made in this project will be loaded to a CD, where it will be available as a showcase.

## 5.1 Hardware

As explained in *Appendix II - Lift and power experiment* the experiment involves the usage of a motor and a propeller to calculate the thrust per power input at a certain angular velocity. These data can be used to find the power the system requires to hover. The set-up of the experiment is described in *Appendix II - Lift and power experiment*. The power loss due to the components in the system is taken into account in the measured data. These components are the motor, the ESC, and in the *Arduino* system. Thus, the losses are already accounted for in the data sets, without the battery losses though. Because the battery is not taken into account in the experiment, its quantities need to be added to the data.

A battery will discharge over time and have an internal resistance. The internal resistance varies with the battery type and so does the discharge rate. These factors are not given

by the manufacturers. Because these factors are unknown the losses from the battery is assumed to be 10 %. This section will demonstrate how the hover time is calculated using data from experiment *Appendix II - Lift and power experiment* with a set-up consisting of a motor of the type *Turnigy Multistar 1704-1900Kv*, a propeller of the type *GWS EP 7035*, and a battery of type *Lipo Receiver Pack 2200mAh battery Digi-Power, 7,4 V*. The masses of the main components are outlined in table 5.1.

	Mass (g)
Motor	$13,5 \times 4 = 54$
Propeller	$5 \times 4 = 20$
Battery	114
Frame	90
Black box	50
<b>Total</b>	<b>328</b>

Table 5.1: Weight of the system components.

## 5.2 Hover time of a quadcopter

Each motor needs to lift one fourth of a quadcopter. The force required to hover can be found by fitting the experimental data (for one motor) in a polynomial of second degree regression (by 4.45,  $F_t = b\omega^2$ ). Figure 5.2 illustrates this. Thus, the angular velocity ( $\omega$ ) can be found for this required force.

The Thrust and angular velocity from the experiment *Appendix II - Lift and power experiment* is illustrated by figure 5.2.

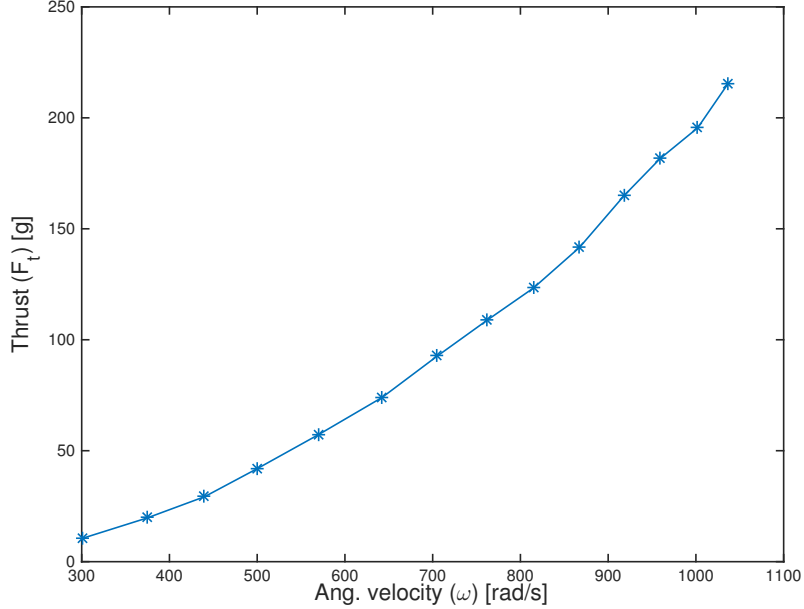


Figure 5.2: The relation between the angular velocity and the thrust.

The thrust illustrated by the graph in figure 5.2 needs to be a fourth part of the total

weight of the quadcopter, because the quadcopter consists of four sets of motor/propeller, which all need to produce an equal amount of lift force. The *Arduino* program collects weight measurements of the motor/propeller set up and resets the lift. The data from the *Arduino* program can then be converted into lift mass per power input. The relation between the angular velocity and the lift mass per power input can be seen on figure 5.3. Based on this the lift mass per power input ( $\text{g}/\text{W}$ ) can be found as a function of the angular velocity. This is shown by figure 5.3.

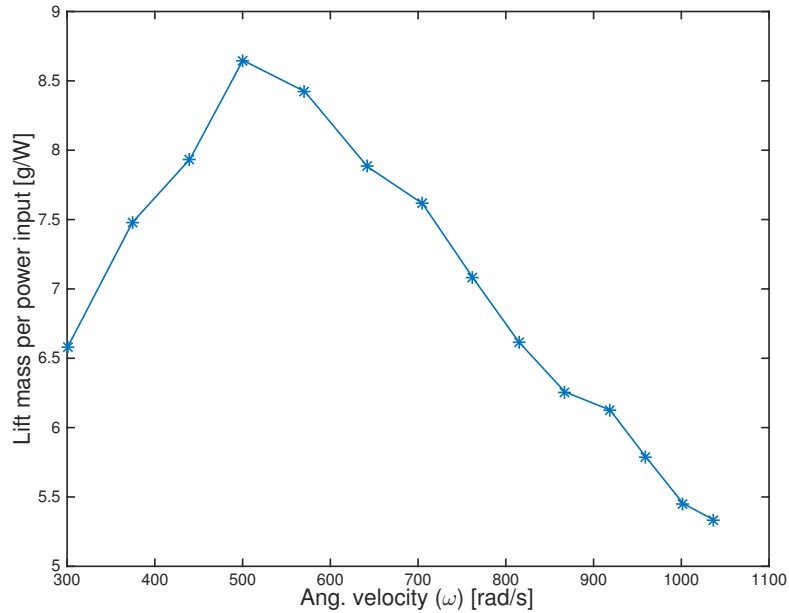


Figure 5.3: The relation between the angular velocity [rad/s] and the lift per watt [ $\text{g}/\text{W}$ ].

When the lift mass per power input is known, the power consumption of each motor can be found by dividing the weight each motor have to lift by the lift mass per power input. The amount of energy the battery is able to store can be found by multiplying its capacity with the voltage across its terminals. The battery energy divided by the power equals the hover time.

The mass of the frame and black box are estimated values. The mass of the remaining main components are known. This gives a total mass of the quadcopter of 328 g. This means that each motor/propeller set needs to produce a thrust capable of lifting 82 g. Since one motor weighs 13,5 g, each of the four motors have to lift around six times their own weight to be able to hover in this set-up.

### 5.2.1 Hover time

To find an approximated hover time, the power and the thrust the quadcopter requires to hover will be determined by calculations based on the experimental data sets. By equation 4.45,  $F_t = b\omega^2$ , it can be seen that the approximation needs to be a polynomial fit. Figure 5.4 illustrates this.

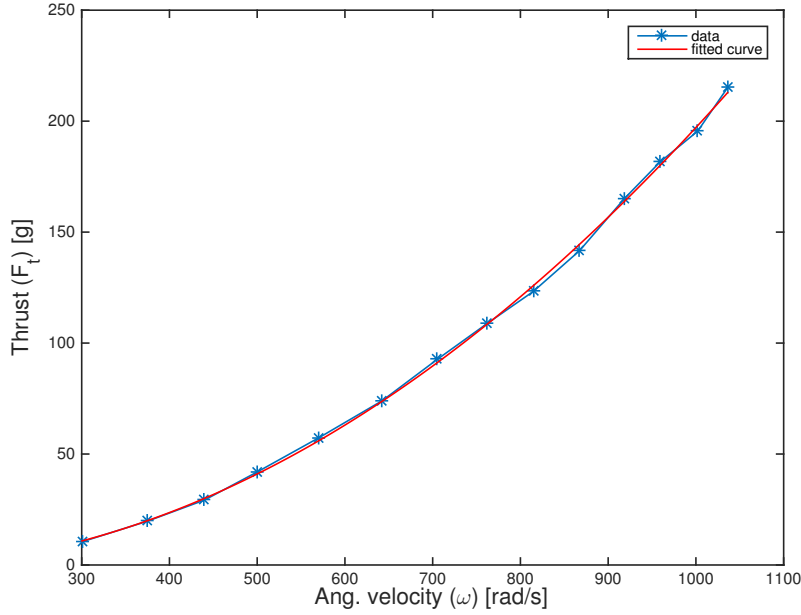


Figure 5.4: Thrust as a function of the angular velocity.

The equation for the fitted curve is given by equation 5.1.

$$F_t = 2,4105 \cdot 10^{-4} \cdot \omega^2 - 0,0540 \cdot \omega - 0,0133 \quad (5.1)$$

The *R-square* for the regression is 0,9984 <sup>1</sup>. If the weight, each motor needs to lift, is inserted in equation 5.1, it yields the angular velocity required to hover. Each motor/propeller set need to lift 82 g in this system. To be able to hover, it will require an angular velocity at 682 rad/s (see figure 5.5). To clarify, if another frame or battery were used the angular velocity would be different.

---

<sup>1</sup>The closer  $R^2$  gets to 1, the closer the approximated function is to the real data set, where 1 is the exact function.

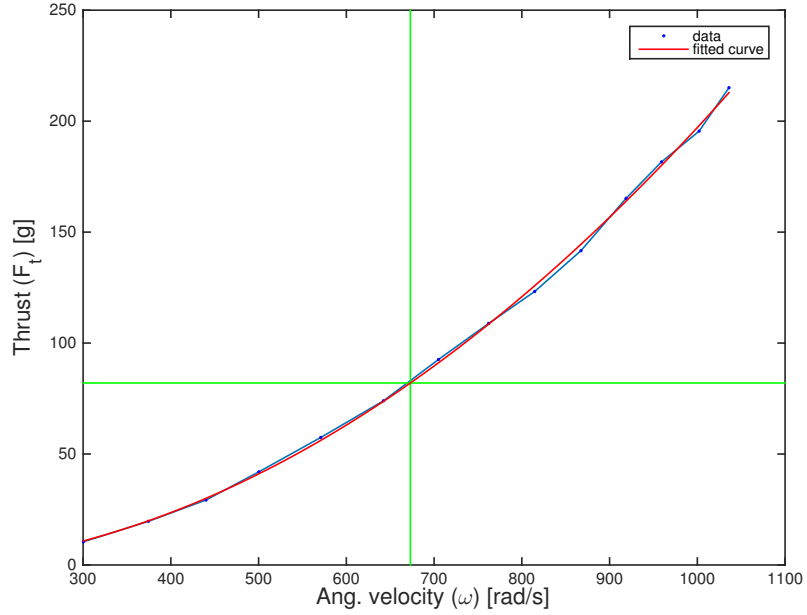


Figure 5.5: Thrust over RPM with a load point calculated

With the angular velocity from the data set given, the lift mass per power input can be found. This can be used to find the total amount of power the system uses to hover. The best approximation for the lift mass per power input as a function of the angular velocity is a polynomial regression. The CEMF will increase as the angular velocity increases, thus reducing the internal ohmic power losses (see equation 4.13). However, the drag force and the power losses in the iron bearings will increase as the angular velocity (see equation 4.15). The fit for this equation will consequently be a polynomial equation. The data set for this is shown by figure 5.6 along the fitted curve.

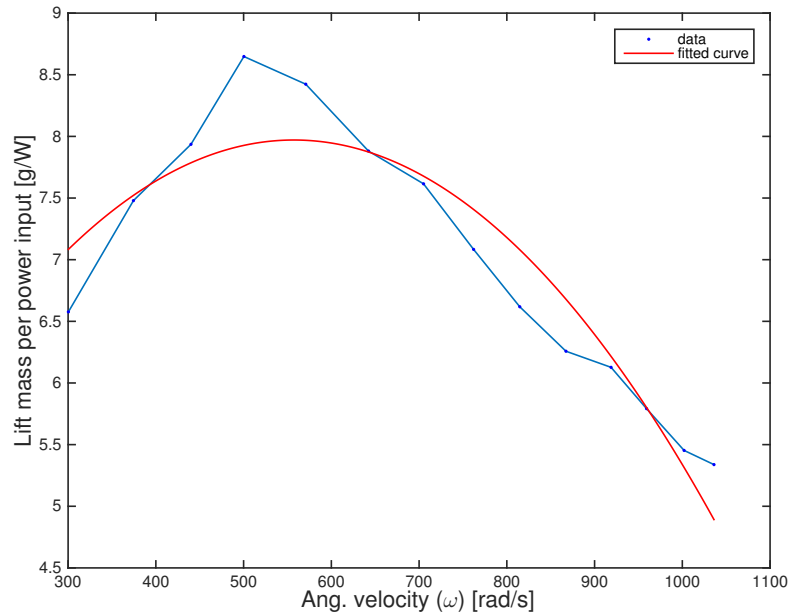


Figure 5.6: Gram per watt over RPM with fitted curve

The expression for the fitted curve is given by equation 5.2.

$$f(\omega) = -1,8350 \cdot 10^{-5} \omega^2 + 0,0256\omega - 1,9028 \quad (5.2)$$

It can be seen on figure 5.6 that there some deviation, which makes the fit less accurate ( $R\text{-square} = 0,8625$ ). By using the specific angular velocity, which is needed to hover, the lift mass per power input can be found. Figure 5.7 shows the angular velocity is set to 673 rad/s, and the lift mass per power input can be seen by figure 5.7.

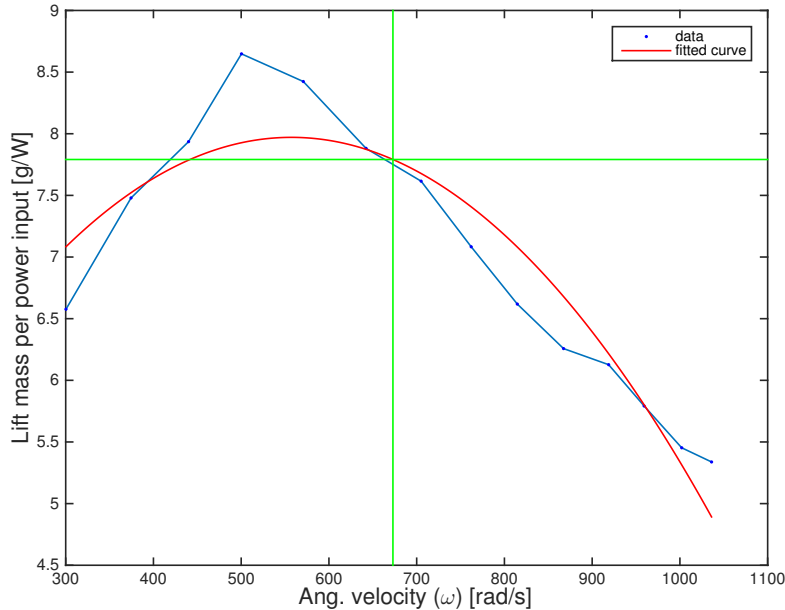


Figure 5.7: Gram per watt over RPM with a load point calculated.

Thus, it can be seen that to lift 82 g per motor, it requires the motors to operates at 673 rad/s. The lift grams to power ratio is 7,79 g/W. Hence, the total amount of power consumed by the system can be calculated as in equation 5.3.

$$\frac{82g}{7,79g/W} \cdot 4 = 42,09W \quad (5.3)$$

Thus, the total power consumption of the system is 42,09 W.

This leads to the battery, which have an amount of energy stored. Regular batteries have a given voltage across its terminals and an energy capacity. With a voltage of 7,4 V and a capacity of 2.200 mAh the total amount of energy is calculated by equation 5.4 and 5.5 giving  $7,4V \cdot 1,98Ah = 14,65Wh$ .

$$7,4V \cdot 1,98Ah = 14,65Wh \quad (5.4)$$

$$\frac{14,65Wh}{42,09W} = \frac{14,65Wh \cdot 3.600}{42,09W} = 1.253s \quad (5.5)$$

The equations yields a hover time of 1.253 second, which is 20 minutes and 53 seconds.

## Adjustable number of motors

An option could be adjusting the amount of motors on the quadcopter to see, whether it increases or decreases the flight time. Less motors will use less power and have a smaller weight, which would require a smaller lift, but fewer motors will also produce a lower lift. Since the weight of the motor is small compared to the whole system, continuously decreasing the number of motors will not necessarily increase the flight time. A higher number of motors would create more lift, but also consume more power. In addition, this means that continuously increasing the number of motors eventually would result in a decrease of the flight time. Based on the test data a optimum number of motors is calculated, using the same variables for the mass and the battery. The only varying masses would be the motor weight of 13,5 g, the propeller weight of 5 g, and the frame mass of 90 g. The script has simulated the hover time with a different amount of motors, which can be seen by figure 5.8. In these simulations it is estimated that each rod weighs 10 g, and the centre 50 g. This is not an accurate assumption, because the dimensions of the frame will slightly differ for each simulation, due to the structure and dimensions would change.

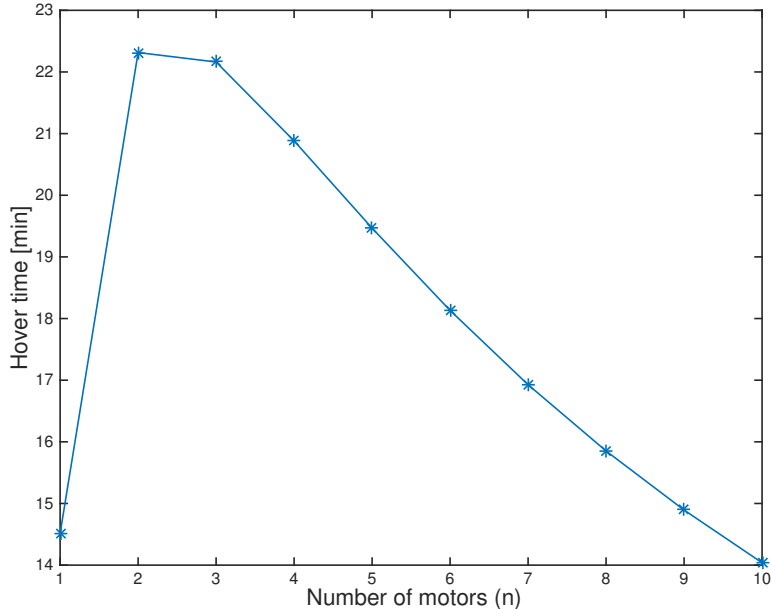


Figure 5.8: Number of motors with their respective flight time

On figure 5.8 it can be seen how operating with two or three motors is the best option according to the data from the experiments. Hence, the longest hover time is achieved. As seen by figure 5.8 the hover time is about 22 minutes in both cases, with the two motor system having the longest hover time. Arguments against using a two or three motored multicopter can be the fact that a quadcopter (four motored) is easier to control. Thereby, the quadcopter is still the best option.

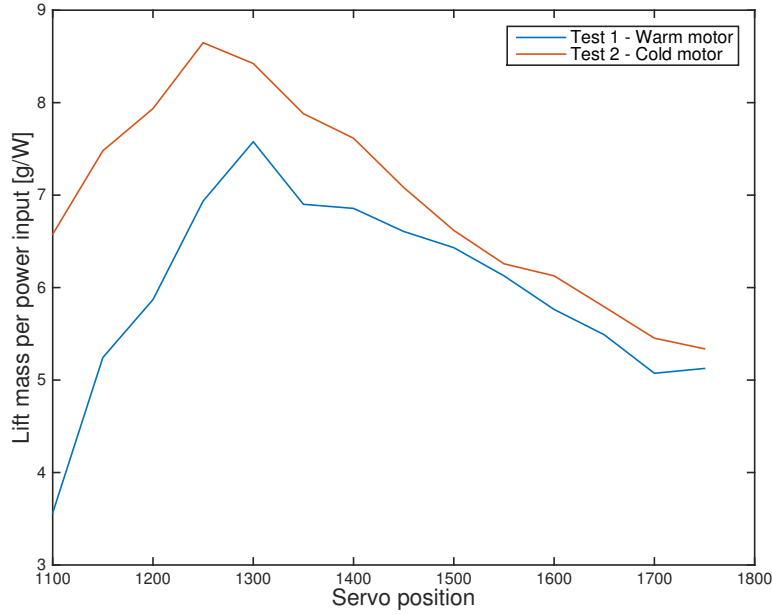


Figure 5.9: Simulation with an octocopter with needed thrust and g/W load points

On figure 5.9 a simulation with eight motors and propellers has been made. Notice how the load point for eight motors is lower than the load point for four motors, see figure 5.9. Since eight motors is used, a greater amount of power is required. This is why the flight time is only 15 minutes and therefore not very efficient.

The approximated hover time for a quadcopter can be found from experimental data. It requires an experiment with a motor/propeller set-up as in the *Appendix II - Lift and power experiment*. The power consumption, the lift from the propeller and the angular velocity have to be measured. From this data, the hover time can be calculated by choosing a the rest of components such as frame (which provides an additional mass), a suitable battery for the motor/propeller together with the additional mass of the black box. If another frame or battery is wanted it can easily be changed in the MatLab-script.

### 5.3 Determination of the power losses of the system

In order to determine the efficiency of the motor/propeller system, the power losses of the system must be known. These quantities is the drag force, the friction caused by the bearings, the dry friction, and the losses due to the moment of inertia.

The power output is given by equation 5.6.

$$P_{out} = \tau_{em} \cdot \omega \quad (5.6)$$

The electromechanical torque,  $\tau_{em}$  is assumed to be expressed by equation 5.7.

$$\tau_{em} = B\omega^2 + B_v\omega + \tau_{dry} + J \cdot \frac{d\omega}{dt} \quad (5.7)$$

To determine these coefficients, the electromechanical torque is set to zero. This is achieved by letting the motor operate in cut-off mode (it is disconnected from the input power

source), and the servo position is brought to idle. Hence, the motor slows down and stops. The torque due to the moment of inertia makes the propeller rotate for a short period of time. The torque due to the moment of inertia can be expressed by equation 5.8.

$$0 = B\omega^2 + B_v\omega + \tau_{dry} + J \cdot \frac{d\omega}{dt} \iff -J \cdot \frac{d\omega}{dt} = B\omega^2 + B_v\omega + \tau_{dry} \quad (5.8)$$

Thus, by determining the characteristic of equation 5.8, the constants  $B$ ,  $B_v$ , and  $\tau_{dry}$  can be found.

The CEMF is measured by connecting the oscilloscope to the terminals of the motor through a differential probe. The data is shown in figure 5.11.

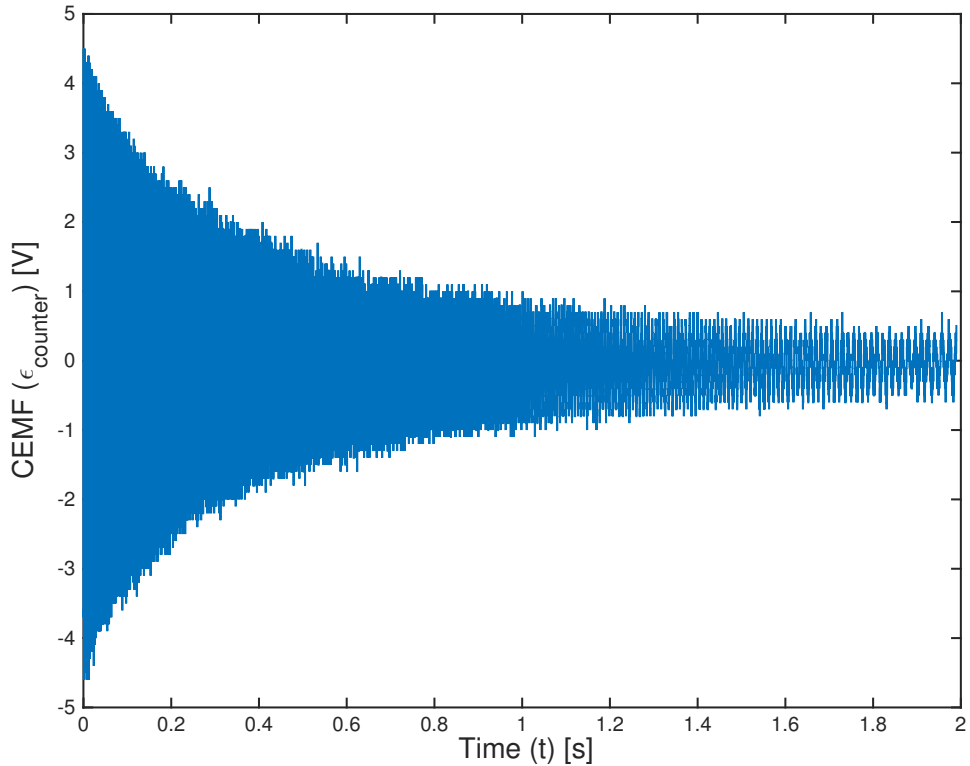


Figure 5.10: The graph shows the raw data of the CEMF as a function of time, when the motor the operation in cut-off mode.

It can be seen by figure 5.10 that the magnitude of the CEMF is decreasing. In order to determine the characteristic of the expiration time, only the positive peak points are analyzed. These are plotted in figure 5.11.

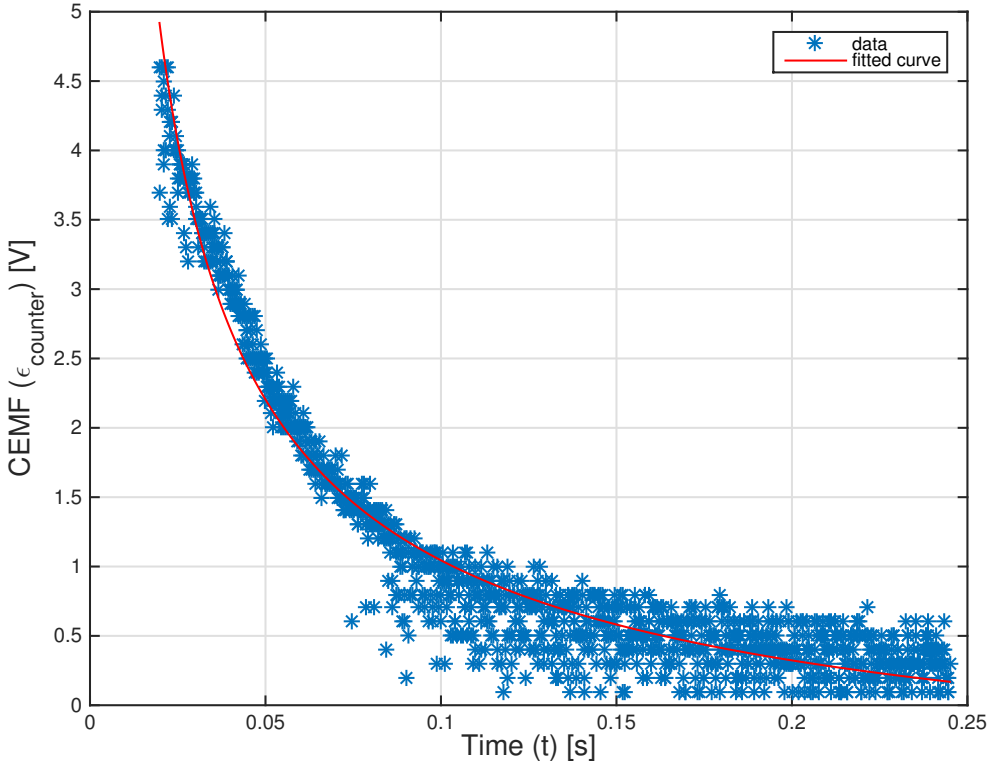


Figure 5.11: The graph shows a characteristic of the CEMF generated as a function of time, when the motor is operating in cut-off mode.

Because the CEMF is proportional to the angular velocity (see equation 4.13), and angular velocity is inverse proportional to time ( $\omega = 2\pi t^{-1}$ ), it is reasonable to assume that the best fit would be power regression. Thus, the fitted curve over the data is made by power regression with an *R-square* of 0,9339, and expresses the induced EMF as a function of time and is shown by equation 5.9.

$$\varepsilon(t) = 0,08929 \cdot t^{-1,044} \quad (5.9)$$

Due to the relation between CEMF and angular velocity is given by  $\varepsilon = K_\varphi \omega$ , an expression for the angular velocity as a function of time can be determined by rewriting 5.9 in terms of the angular velocity.

$$0,08929 \cdot t^{-1,044} = K_\varphi \cdot \omega \iff \omega = \frac{0,08929 \cdot t^{-1,044}}{K_\varphi} \quad (5.10)$$

The CEMF-constant is found by the values of the angular velocity,  $\omega_{ss}$ , and the CEMF,  $\varepsilon_{ss}$ , measured just before the motor enters cut-off mode (operating in steady state (ss)).

$$K_\varphi = \frac{\varepsilon_{ss}}{\omega_{ss}} \implies \frac{4,6V}{989,57 \frac{rad}{s}} = 0,004648 \frac{V \cdot s}{rad} \quad (5.11)$$

By inserting the value of  $K_\varphi$  in equation 5.10, the angular velocity as a function of time can be expressed.

$$\omega(t) = \frac{0,08929 \cdot t^{-1,044}}{0,004648} \implies 19,21 \cdot t^{-1,044} \quad (5.12)$$

The graph for  $\omega(t)$  is drawn in figure 5.12, along with the corresponding data set, which is derived from the data set over the EMF by multiplying with  $K_\varphi$ .

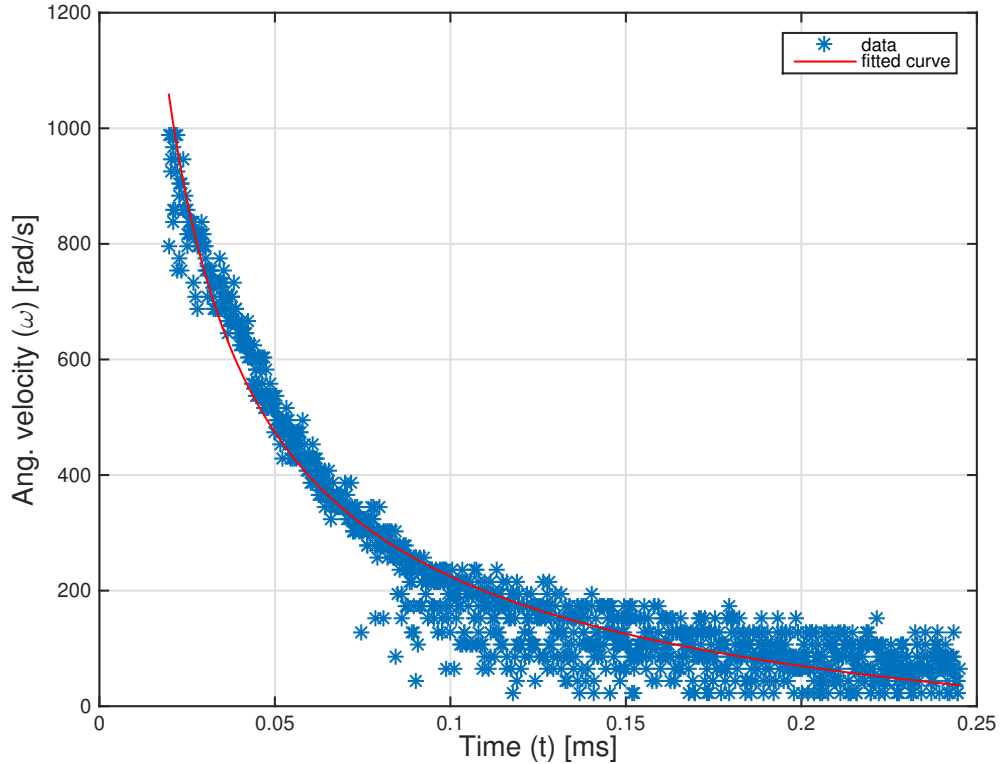


Figure 5.12: The graph shows a characteristic over the angular velocity as a function of time, when the motor the operation in cut-off mode.

By differentiating equation 5.12 with respect to time, it yields the change in angular velocity (angular acceleration).

$$\frac{d\omega}{dt} = 20,05524 \cdot t^{0,044} \quad (5.13)$$

The moment of inertia,  $J_{total}$ , for a propeller with thickness,  $h$ , can be described as a planform area (as described in *Mechanical losses*), see equation 5.15.

$$J = \frac{1}{12} \rho \cdot h \cdot l \cdot w \cdot (l^2 + w^2) \quad (5.14)$$

Here  $l$  is length of the propeller,  $w$  is the average width, and  $\rho$  is the density. The propeller of type *GWS EP 7035* with two blades has a diameter of 176 mm, a thickness of 1 mm, an average width of 13,5 mm, and a density of  $930 \frac{kg}{m^3}$ .

$$J = \frac{1}{12} \cdot 930 \frac{kg}{m^3} \cdot 0,001m \cdot 0,176m \cdot 0,0135m \cdot ((0,176m)^2 + (0,0135m)^2) = 7,298 \cdot 10^{-7} kg \cdot m^2 \quad (5.15)$$

This means that the moment of inertia for the propeller is about  $7,298 \cdot 10^{-7} kg \cdot m^2$

By multiplying equation 5.13 with the value of the moment of inertia, the data set, the expression for the torque due to the moment of inertia can be found. This is done by

multiplying each entry of the matrix of the data set with the product of the moment of inertia and the expression for the angular velocity. Thus, the torque due to the moment of inertia can be found as a function of the angular velocity, see figure 5.13.

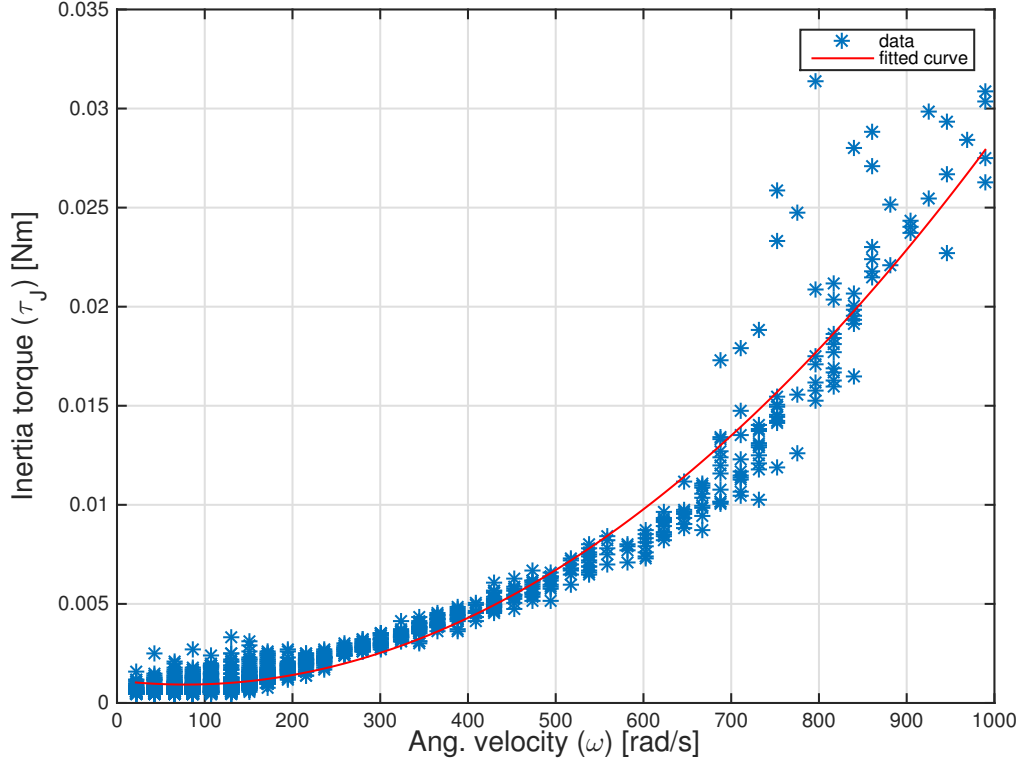


Figure 5.13: A characteristic over the angular velocity as a function of time, when the motor is operating in cut-off mode.

Due to equation 4.21, the relation between the angular velocity and the torque produced by the moment of inertia is quadratic, thus making a polynomial fit with two arguments a desired method to determine an expression for torque due to the moment of inertia as a function of the angular velocity. It yields:

$$\tau_J(\omega) = 4,9707 \cdot 10^{-8} \cdot \omega^2 - 1,4438 \cdot 10^{-5} \cdot \omega + 0,0016 \quad (5.16)$$

The values of the constants  $B$ ,  $B_v$ , and  $\tau_{dry}$  are explicitly expressed by equation 5.16.

- $B = 4,9707 \cdot 10^{-8} \frac{Nms^2}{rad}$
- $B_v = -1,4438 \cdot 10^{-5} \frac{Nms}{rad}$
- $\tau_{dry} = 0,0016 Nm$

These coefficients represent the power losses due to different factors, which affect the system. By inserting these consist in the expression of the electromechanical torque (equation 4.21, it yields the following approximated expression:

$$\tau_{em}(\omega) = 4,9707 \cdot 10^{-8} \cdot \omega^2 - 1,4438 \cdot 10^{-5} \cdot \omega + 0,0016 + 7,29769 \cdot 10^{-7} \cdot \frac{d\omega}{dt} \quad (5.17)$$

Since the constants in equation 4.21 are valid for all values of the angular velocity of the motor a descending set of angular velocities has been created and used to calculate the torque. This was done to match the data from the first test *Lift and power*. The torque was then plotted over the angular velocity, see figure 5.14.

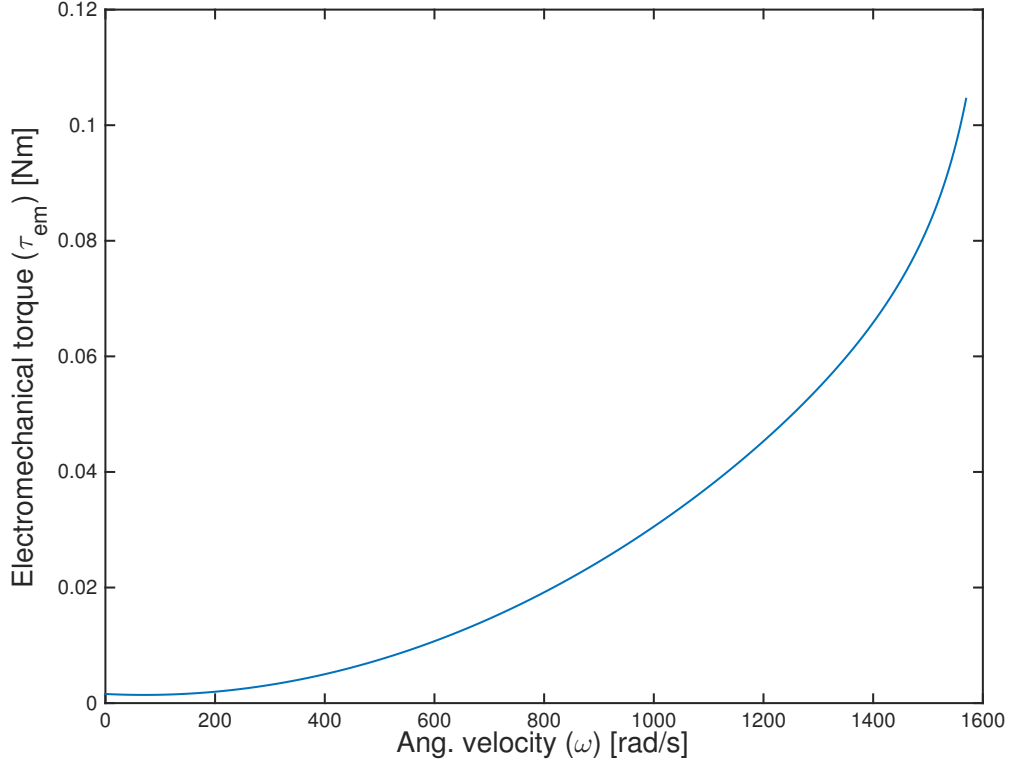


Figure 5.14: The electromechanical torque as a function of the angular velocity.

Figure 5.14 illustrates the angular velocity as a function of electromechanical torque.  
2

## 5.4 Efficiency of the system

The efficiency of the motor is given by the ratio of the mechanical power output and the electrical power input. The efficiency of the system (when operating in steady state, where  $\tau_J$  and  $\tau_{dry}$  are zero) can be expressed by equation 5.18.

$$\eta = \frac{\tau \cdot \omega}{I \cdot (U_{motor}) - (\tau_B \omega + \tau_{Bv} \omega)} \quad (5.18)$$

Figure 5.15 plots the calculated output power and the measured angular velocity.

---

<sup>2</sup>Approach and equipment used during this experiment can be seen in *Appendix III - Mechanical losses - experiment*.

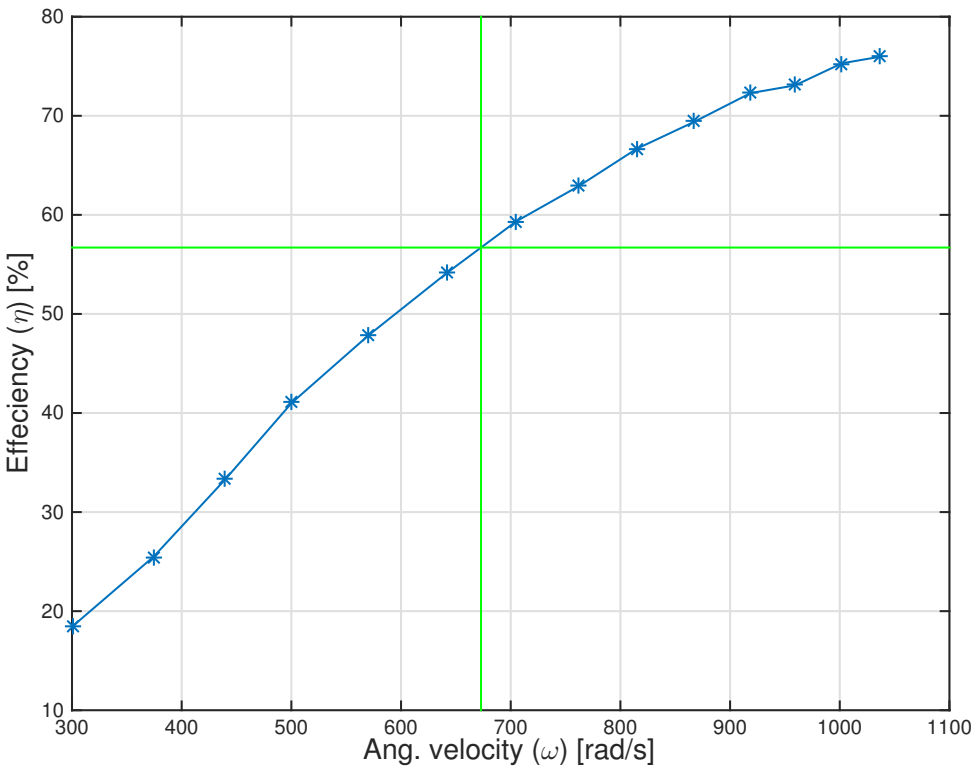


Figure 5.15: The graph shows the efficiency of the motor as a function of the angular velocity.

As illustrated by figure 5.15 the efficiency of the system increases with the angular velocity. The characteristic of the graph corresponds to the fact that when the angular velocity increases, the efficiency increases as well, due to the induced CEMF. At low velocities, the efficiency is only about 30 % and at higher velocities is around 70 %. The highest efficiency is achieved at 991 rad/s where the efficiency is 78,8 %. Comparing this to the best operating point for the propeller tested as load, the best load point for four motors is 671 rad/s. It can be argued that, it is desirable to have the highest possible efficiency, but since it depends on the angular velocity, and due to the fact that an increase of the rated velocity would reduce the rated electromechanical torque, thus plausibly reducing the amount of lift. Hence, a high efficiency does not necessarily equally correspond to a higher thrust to power ratio.

# 6 | Evaluation

In the following section, the characteristics and the results of *Characteristics of a motor and propeller system*, are evaluated. Furthermore, the validity of the results, derived from the data sets, will be considered.

## 6.1 Data sets

The motor (*Turnigy Multistar 1704 1900 Kv*) was tested two times on two separate days, one where the motor had been running, thus a temperature limitation regarding the internal resistance may have occurred. The second test was done with a cold motor. Based on the results, it seems that the motor operates better, when it is not preheated.

As seen in figure 5.2 and 5.3, it seems that there is some few off measurement around 600 rad/s. This can be inaccurate data, though this is improbable since the test data show that on two separate dates, the separation points are at the same angular velocity. This means the motor operates best to that specific load point. Because of the deviation for the fitted curve in figure 5.7, the polynomial fit is not as accurate. Two tests were made when measuring the thrust as a function of the angular velocity over two days, further explained in *Appendix II - Lift and power experiment*. The first test was measured with the motor at a higher temperature where as the second test the following day was made with a motor at a lower temperature. This temperature difference could have had an influence on the efficiency of the motor.

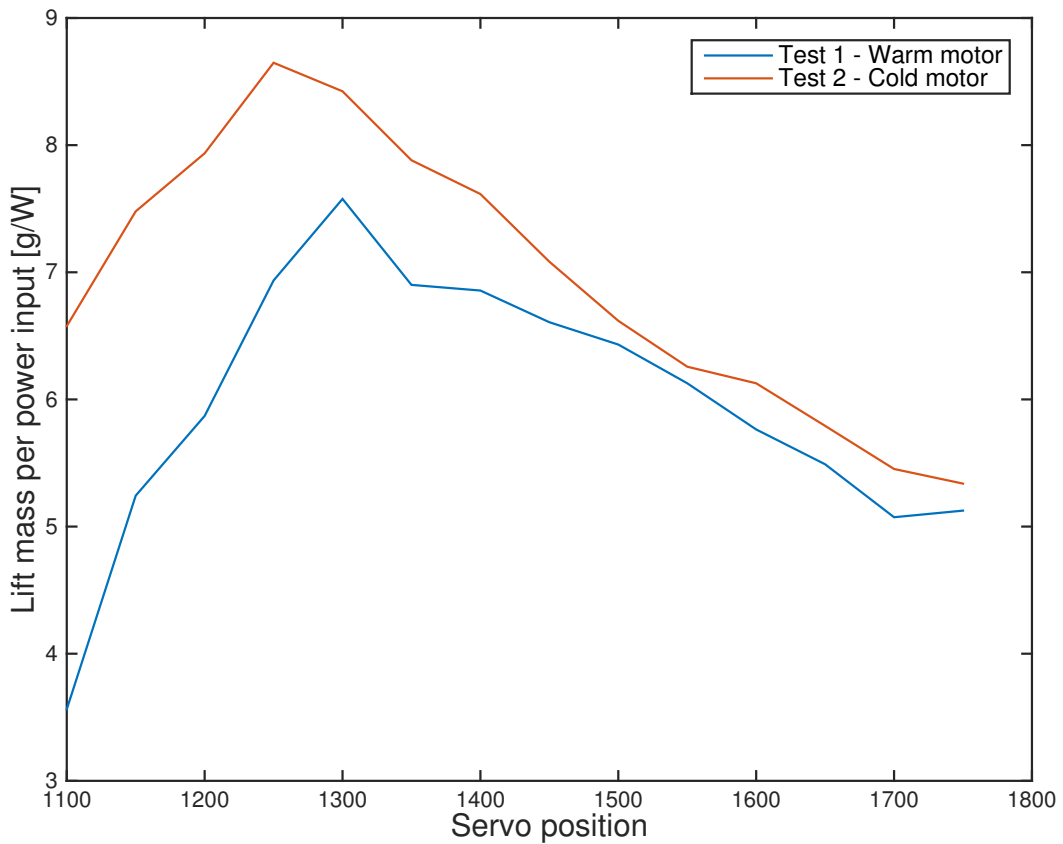


Figure 6.1: The difference between the servo position and the gram per watt [g/W] for the 2 separate data sets.

Figure 6.1 shows that the second test (orange) has a much higher lift mass per power input than the first. The deviation is calculated for every 14 entries of the data sets, see table 6.1

Deviation [%]
45,8254
29,8972
26,0290
19,8000
10,0479
12,4380
9,9660
6,7207
2,8218
2,0826
5,9249
5,2145
6,9588
3,9799

Table 6.1: Deviation of each data point of the gram per watt for the 2 test

If the mean value of this matrix is calculated, the mean deviation is about 13 %. This means that the motor was operating at a 13 % higher rate the second day of testing.

The peak found in figure 5.3 can be due to three things:

- Small data offsets.
- A special point with optimal operation point for this particularly load.
- Greater input power consumption (a motor error of some sort could do this).

As seen in the figure 6.2, the power input does not vary at the same point (around 600 rad/s) as the peak in figure 5.3. Therefore, it is improbable to be caused by a greater power consumption. The data offsets seem unlikely as well, because the peaks are observed in the two separated tests. Thus, the peak must be caused by an optimal operation point for the particularly load.

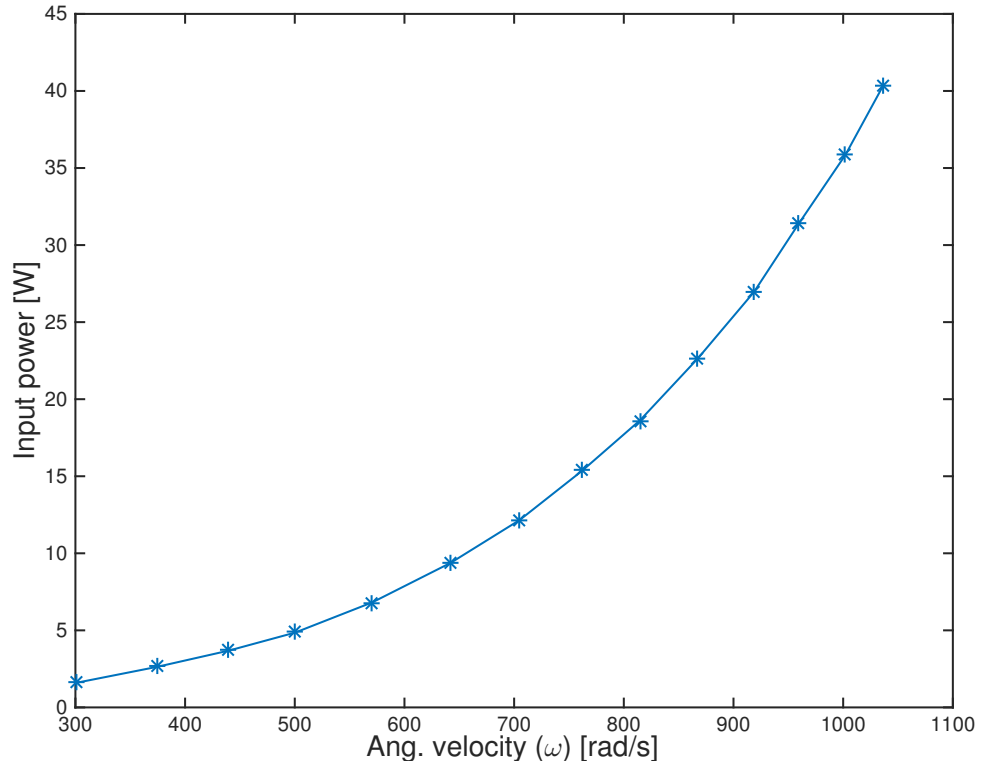


Figure 6.2: Input power in watt over measured rad/s

Since the second test was performed with a motor not preheated, this was the data used for the calculation of the hover time. The difference between the two data sets in hover time with four motors were two minutes in favour of the second data set. A simulation with four motors shows that the hover time would be just under 21 minutes, with a operating point at 671 rad/s.

### 6.1.1 Numerical analysing

In order to get the desired results, the data set has to be analysed numerical. This is performed by plotting the data, and finding the best fitted curve. Since the data

fluctuates around this curve, it is an approximation. Furthermore, numeric differentiation over a particular data set is performed, which is a method to estimate the behaviour of the curve. Since such numeric calculation is performed several times, it is reasonable to assume that the deviation increases. Doing this wrong can easily result in a mix up of the further results and making the calculations and the final result invalid.

## 6.2 Varying numbers of motors/propellers

The best reachable hover time is around 22 minutes, for a motor/propeller set-up of only two, which have been used for testing throughout this project. For the chosen battery and system mass, the optimal number of motors appears to be two in this set-up. The best operating point for the multicopter with two motors is at 842 rad/s. Many different variables in the mathematical model (attached to this project) can be changed, resulting in an increase or decrease of the hover time. Using two or three motors instead of four could also result in difficulties while trying to manoeuvre the multicopter. These difficulties have not been taking into account in the calculations of the model.

The two or three motored options only results in the best option due to the lighter weight. Adding a bigger battery with a slightly bigger capacity and weight would make the quadcopter a better option, hence the weight needed to be lifted by each motor would increase with the number of motors. The load point at rad/s would also increase since more lift mass would be needed.

## 6.3 Efficiency vs. power output

The optimized load point for the propeller used is not operating at most efficient point of the motor. It is possible for a quadcopter to have a high efficiency but still not be able to lift its own weight. Therefore, it is more relevant to look at the lift mass per power input to find the hover time, were the quadcopter weight is included in the considerations, than the energy efficiency.

## 7 | Conclusion

One of the main forces acting on a quadcopter is the gravitational force. In order for a quadcopter to hover it must overcome this natural resistive force with a lift force. In order to create a lift force the propellers have to rotate, which is done by generating a torque. The magnets within the BLDC motor have a magnetic field. The magnetic flux through the area of the current carrying coil generates a magnetic force, which rotates the permanent magnets attached to the rotor and produces a torque.

A quadcopter can only maintain the lift for a certain time period due to the discharge rate of the battery. Quantities like the mass of the components, and the capacity of the battery can be varied in order to affect the hover time. It is also found that the number of motors attached can have an influence on the hover time. The hover time is therefore dependent on the specific choice of main components and a number of motors.

To calculate the hover time and the efficiency of a quadcopter with a certain motor/propeller/battery set-up a mathematical model is made in the program *MatLab*. The mathematical model is described in *Appendix IV - Matlab scripts* and is uploaded to a CD attached to this project. Many different variables in the mathematical model (attached to this project) can be changed, resulting in an increase or decrease of the hover time. Using two or three motors instead of four could also result in difficulties while trying to manoeuvre and accelerate/decelerate the multicopter. These difficulties have not been taking into account in the calculations of the model.

The best reachable hover time is around 22 minutes, with a two motor/propeller set-up, which have been used for testing throughout this project. For the chosen battery and system mass, the optimal number of motors is two. The best operating point for the multicopter with two motors is at 842 rad/s.

The hover time for a quadcopter with a motor/propeller matching the set-up used in chapter *Characteristics of a motor and propeller system* have a hover time about 21 minutes, when operating in steady state (at 671 rad/s) and have an efficiency about 56,7 %.



# 8 | Perspective

This project focuses on finding the hover time and the efficiency of the quadcopter. The following chapter will introduce methods and characteristics, which could have been made if more time was available for this project.

## 8.1 Operating point

This project is only analysing a quadcopter in steady state. If it were to include manoeuvrability (pitching) or accelerating/decelerating, it would have been a more complex and realistic simulation of a quadcopter. The hover time of the quadcopter, which is given by Characteristics of a motor and propeller system, is not the actual hover time. The hover time also depends on how the motor accelerates (starts up). If these advancements were to be included in the model, it would require a system with an alternating and varying current. If the input current to each motor were made controllable in the mathematical model, it would be possible to simulate a quadcopter pitching (turning/manoeuvring) or accelerating/decelerating.

## 8.2 The blade element theory

The lift and drag force of the quadcopter is in this project found experimental. Instead of finding the relations experimental, the blade element theory could have been used to find the lift theoretical. The blade of the quadcopters propeller is divided into small sections. Each blade element have different magnitudes such as the angle of attack (AOA), drag coefficients, width ect. By integrating over the entire blade it will result in a theoretical calculation of the lift forces at different angular velocity. The blade element theory requires that the specific configuration of the propeller is known. This means that the geometry, chord and twist distribution of the quadcopter has to be known in order to use this theory [Latorre, 2011]. The blade element theory could have been used to compare the experimental characteristics of the quadcopters lift with the theoretical.

## 8.3 Torque speed relation

Another characteristic that could have been presented is the torque and angular velocity relation. From this characteristic the maximum mechanical power output can be calculated. Figure 8.1 shows a general model of the torque/speed curve.

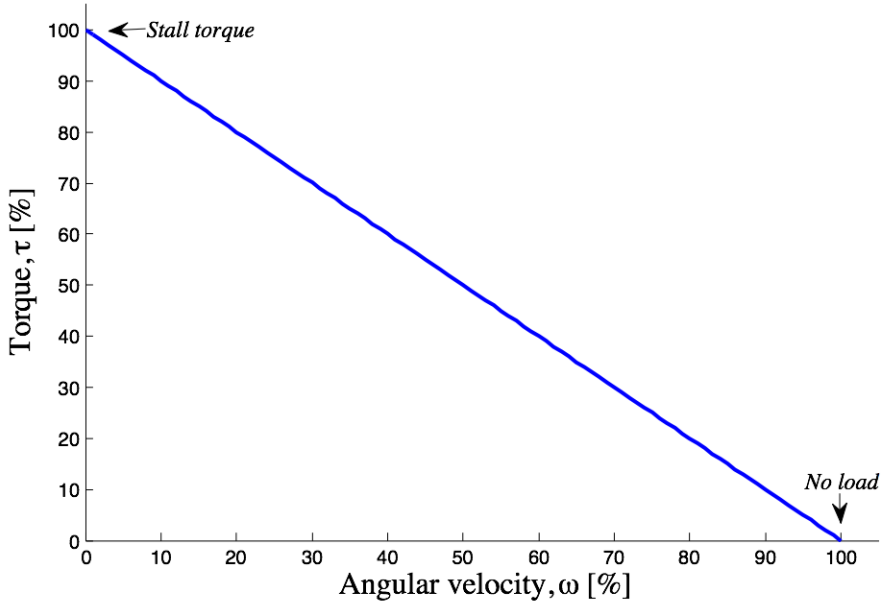


Figure 8.1: A torque/angular velocity curve of a DC motor.

The stall torque,  $\tau_{max}$ , represents the point on the graph, at which the torque is at maximum, but the shaft is not rotating (the motor is blocked). The angular velocity with no load,  $\omega_{max}$ , is the maximum output angular velocity of the motor, and occurs when no load is applied to the output shaft. The mechanical power output can be described as the product of torque and angular velocity. This corresponds to the area of a rectangle under the torque/speed curve with one corner at the origin and another corner at a point on the curve. Any given point on the torque/speed curve represent a point of operation for a motor, but to ensure continuous drift a given motor can be loaded up to a certain torque (any higher load the motor will only be able to operation intermittent). The torque would remain constant for a speed range up to the rated speed, and the mechanical power would increase as the speed increases [Microchip, 2003], [Raymond A. Serway, 2010b].

Due to the linear inverse relationship between torque and angular velocity, the maximum power occurs at the point where the actual torque is  $\frac{1}{2}\tau_{max}$  and the actual angular velocity is  $\frac{1}{2}\omega_{max}$ . This is also illustrated in figure 8.2, where the shaded area under the curve represents the maximum power output.

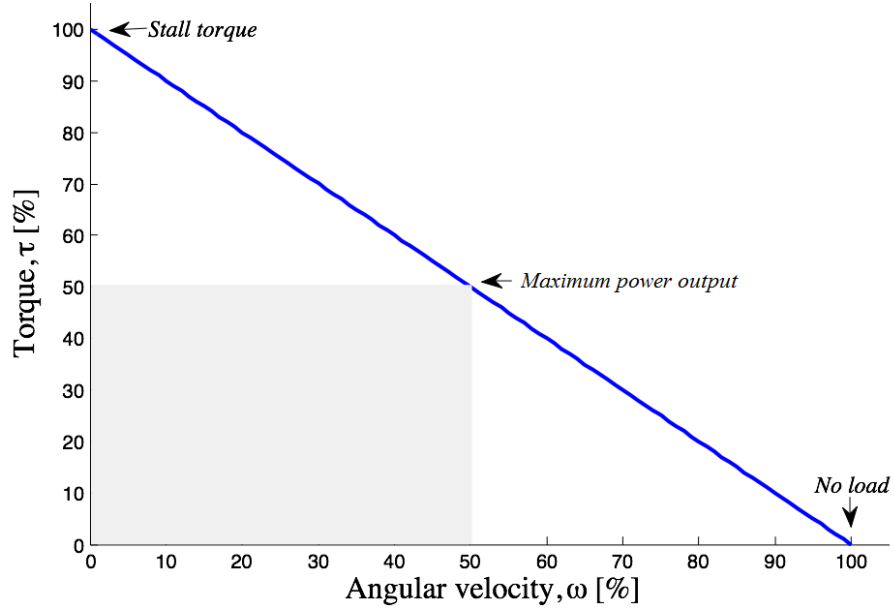


Figure 8.2: It appears that the maximum power output occurs, when the torque and the angular velocity is at 50 % of maximum value.

The actual torque delivered and the actual angular velocity of the motor are given by equation 8.1. This can also be shown analytically by inserting the formula for the actual torque, and angular velocity. The actual angular velocity can be expressed by equation 8.1.

$$\omega = \frac{(\tau_{max} - \tau)}{\tau_{max}} \cdot \omega_{max} \quad (8.1)$$

Inserting equation 8.1 in the expression for the mechanical power output ( $P_{mec} = \tau \cdot \omega$ ), an expression for power as a function of the torque is given.

$$P(\tau) = \frac{\omega_{max}}{\tau_{max}} \cdot \tau^2 + \omega_{max} \cdot \tau \quad (8.2)$$

The maximum power output can then be derived:

$$\frac{dP}{d\tau} = \frac{\omega_{max} \cdot \tau}{\tau_{max}} + \omega_{max} \cdot \tau = 0 \Rightarrow \tau_{mp} = \frac{1}{2} \cdot \tau_{max} \quad (8.3)$$

Thus, the maximum power output occurs, when the torque ( $\tau_{mp}$ ) is half of the maximum torque ( $\tau_{max}$ ) [Page, 1999], as seen on figure 8.2.



# Bibliography

- BLDC wikidot.** BLDC wikidot. *Three Phased Motor*. URL  
[http://bldc.wikidot.com/local--resized-images/bldc-and-8051/Three\\_phase\\_BLDC\\_internal\\_diagram.jpg/medium.jpg](http://bldc.wikidot.com/local--resized-images/bldc-and-8051/Three_phase_BLDC_internal_diagram.jpg/medium.jpg).
- Bright Hub Engineering, 05 2011.** Bright Hub Engineering. *Why Electric Motors Generate Reverse Electromotive Force*, 2011. URL <http://www.brighthubengineering.com/machine-design/75825-do-you-know-why-electric-motors-generate-reverse-electromotive-force/>.
- Cengal A. Yunus, 2012.** Cengal A. Yunus. *Fundamentals of Thermal-Fluid Sciences*. McGraw-hill Education, 2012. Chapter 13, 15.
- Corporation, 2011.** NMB Technologies Corporation. *BLDC Motor & Brushless DC Motor Introduction*, 2011. URL [http://www.nmbtc.com/brushless-dc-motors/engineering/brushless\\_dc\\_motors\\_engineering/](http://www.nmbtc.com/brushless-dc-motors/engineering/brushless_dc_motors_engineering/).
- D. Baert, 1999.** A. Vervaet D. Baert. *Lead-acid battery model for the derivation of Peukert's law*. PERGAMON, 1999.
- Dussault, 03 2014.** Joseph Dussault. *7 commercial uses for drones*. Boston Business, 2014. URL <http://www.boston.com/business/2014/03/14/commercial-uses-for-drones/dscS47PsQdPneIB2UQeY0M/singlepage.html>.
- Embedded, 2014.** *Embedded*. 2014. URL  
<http://www.embedded.com/design/mcus-processors-and-socs/4007628/Designing-a-MCU-driven-permanent-magnet-BLDC-motor-controller-Part-1>.
- Eric Wahl, February 2014.** Sylvee Walenczewski Eric Wahl. *Brushless DC Motors*, Santa Clara University, February 2014.
- Finkbuilt, 06 2014.** Finkbuilt. *Micro FPV Feature on BoingBoing*, 2014. URL  
<http://www.finkbuilt.com/blog/>.
- Gade, 09 2014.** Henrik Gade. UAS-Works, 2014. Opfinder gruppe.
- Garage, 2014.** *Quadcopter Garage*, 2014. URL <http://quadcoptergarage.com/diy-quadcopter-build-part-one-planning-parts-list/>. Picture.
- Gibiansky, November 2012.** Andrew Gibiansky. *Quadcopter Dynamics and Simulation*. 2012. URL  
<http://andrew.gibiansky.com/blog/physics/quadcopter-dynamics/>.

**Griffiths, 12 2013.** Sarah Griffiths. *Now DHL tests a delivery drone: Airborne robots could be used to deliver medicine to hard-to-reach places*, 2013. URL  
<http://www.dailymail.co.uk/sciencetech/article-2520818/DHL-tests-delivery-drone-airborne-robots-used-deliver-medicine.html>.

**Intech.** Intech. URL  
<http://www.intechopen.com/source/html/16242/media/image8.png>.

**Karadimov, April 2000.** Andrey Karadimov. *Electromechanical systems - Brushless DC Motors*, 2000. URL  
[http://educypedia.karadimov.info/library/ems\\_ch12\\_nt.pdf](http://educypedia.karadimov.info/library/ems_ch12_nt.pdf). Based on lectures from University of technology, Sydney - facility of engineering. Lecturers: Dr. Peter Watterson and Prof. Joe Zhu.

**Latorre, June 2011.** Eva Saade Latorre. *Propulsion system optimization for an unmanned lightweight quadrotor*. 2011. URL  
<http://upcommons.upc.edu/pfc/bitstream/2099.1/12472/1/memoria.pdf>.

**Lauszus.** Lauszus. *Guide to gyro and accelerometer with Arduino including Kalman filtering*. URL <http://www.instructables.com/id/Guide-to-gyro-and-accelerometer-with-Arduino-inclu/>.

**Lyle, 09 2010.** Tech. Sgt. Amaani Lyle. *Unmanned Aerial Vehicle*, 2010. URL  
<http://archive.today/20120719164359/http://www.af.mil/news/story.asp?storyID=123208561>.

**MatLab.** Simulink MatLab. *DC Motor Speed: Simulink Modeling*.

**Microchip, 2003.** Microchip. *Brushless DC (BLDC) Motor Fundamentals*. 2003. URL  
<http://www.mouser.com/pdfdocs/BrushlessDCBLDCMotorFundamentals.PDF>.

**Mikael Cugnet, Matthieu Dubarry, 2010.** Bor Yann Liaw Mikael Cugnet, Matthieu Dubarry. *Peukert's Law of a Lead-Acid Battery Simulated by a Mathematical Model*, 2010.

**Page, 1999.** Matt Page. *Understanding D.C. Motor Characteristics*. 1999. URL  
<http://lancet.mit.edu/motors/motors3.html>.

**Pyramid models.** Pyramid models. *HK TALON Quadcopter Frame*. URL  
[http://www.pyramidmodels.com/shop/product.php/922/hk\\_talon\\_quadcopter\\_frame\\_multicopter\\_kkboard](http://www.pyramidmodels.com/shop/product.php/922/hk_talon_quadcopter_frame_multicopter_kkboard).

**Raymond A. Serway, John W. Jewitt, 2010.** Jr. Raymond A. Serway, John W. Jewitt. *Physics for Scientists and Engineers with Modern Physics*. Mary Finch, 2010.

**Villasenor, 04 2012.** John Villasenor. *What Is a Drone, Anyway?*, 2012. URL  
<http://blogs.scientificamerican.com/guest-blog/2012/04/12/what-is-a-drone-anyway/>.

**Watkinson, 12 2003.** John Watkinson. *Art Of The Helicopter*. Butterworth Heinemann, 2003.

**Wetzel, 2012.** John Wetzel. *WikiPremed*, 2012. URL [http://www.wikipremed.com/image.php?img=010108\\_68zzz116900\\_18201\\_68.jpg&image\\_id=116900](http://www.wikipremed.com/image.php?img=010108_68zzz116900_18201_68.jpg&image_id=116900). Air flow around an airplane wing.

**Wolfson, 2011.** Richard Wolfson. *Essential University Physics: Volume 1 (2nd Edition)*. Addison-Wesley, 2011.



# Appendices



# Appendix I - Experiment-equipment

## Arduino meseasument

*Arduino* is an open-source, electronics platform based hardware and software. The *Arduino* receives inputs from varies of sensors, control the inputs, and measure the outputs, such as the voltagedrop, lift, and current. *Arduino* is operated by user written code, in the *Arduino* programming language. When a code is uploaded to the hardware it initialized the whole system, starting the test. The software was set-up to take the average of 16 measurements for each printed data point. When initialized all variables were set to zero, letting the motor run up to its starting servo position. Then the servo position increased by  $\pm 10$  every time until a fixed servo position was reached. An example on how coding is written in the *Arduino* software can be seen on 1. The printed data were exported as a normal text file where the measurements were separated by a semicolon, this could then be imported into Matlab.



```
// Serial.println(volt);
// Serial.println("#trust:g/W:servopos:volt:amp:Watt");
//}

//for (pos = 1000; pos < 1700; pos += 10) // goes from 0 degrees to 180 degree
for (pos = 1000; pos < 2000; pos += 10) // goes from 0 degrees to 180 degrees
{ // in steps of 1 degree
if (pos >= fixedPwm){pos = fixedPwm;}
myservo.write(pos); // tell servo to go to position in variable 'pos'
myservo.write(1300);
delay(100); // waits XXms for the servo to reach
servopos = pos;

for (int antal = 0; antal < 10; antal++) {
maalinger();
printdata();
if (volt < StopVolt) {
break;
}
}
maalinger();
if (volt < StopVolt) {
break;
}
}
```

Figure 1: A picture of how code can be written with the *Arduino* software

## Measuring RPM

The only thing that the *Arduino* hardware could not measure was the angular velocity of the propel. This had to be done manually by using one of two methods.

**Stroboscope** Instrument for measuring rotational velocities. A strobe consists of a glow lamp that turns on with very constant time intervals and illuminates the object. If pointed

at a particular marked location on the object, it can be adjusted by the interval of the light, until the rotating object seems to be standing still as the frequency of the light matches the rotation of the object. At this point the rotational velocity can be read off the stroboscope.

**Tachometer** The tachometer works somehow in the same way as the stroboscope, only the tachometer measures the rotational speed with a small laser. This is done by placing reflective tape on the propeller, then each time the laser detects the tape it will record it and state the rotational speed.

Both methods were tested and the results were nearly identical. The difference was  $\pm 3$  RPM when operating around 5000 RPM. Since the tachometer is much easier to use, it was preferred. The stroboscope and the tachometer can be seen on the left by figure 2.

## Equipment test

The purpose of this experiment is to test how the measuring gear works and how to collect the data via the *Arduino*-software. This is done by testing different kinds of motor/propeller combination. Besides testing the set-up, it is desired to find and resolve potential threats that might occur while collecting data. Following measuring variables will be tested:

- The thrust
- The angular velocity
- Voltage drop
- Current input

The power consumption of the motor is being calculated in the program *Arduino*, by using the voltage drop and current input as variables.

## Test set-up

The test consists of a motor and propeller attached on one end on a lever. The other end is attached to a table and is connected to a newton-meter, which measures the thrust. The different variables is measured by using the hardware *Arduino*. The angular velocity (RPM) is measured by a hand-held tachometer or a stroboscope.

Figure 2 shows the test set-up. An ESC are controlling the current input and thereby the RPM of the motor. The program *Arduino* measures the thrust and is calculating the power consumption of the motor by using the voltage drop over the motor and the input current. Furthermore, the collected data is being logged on a computer.

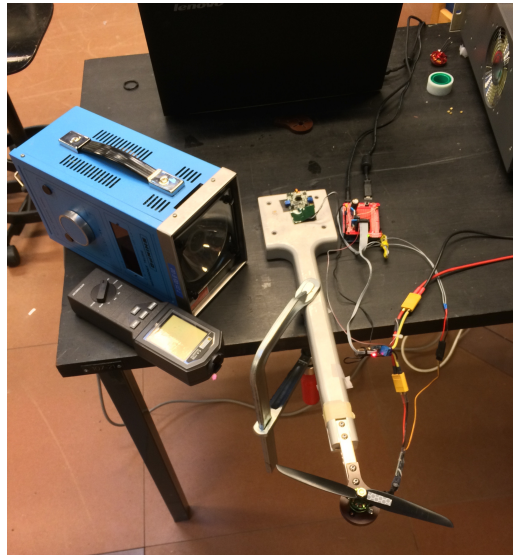


Figure 2: A picture of the test set-up.

## Results and experiment discussion

Experiment 1 showed calibration errors on the newton-meter, which varied results of the thrust by eight grams. The test set-up was then calibrated correctly, so the collected data were reasonable and matching the test situation.

The experiment was also to test how the hardware functions and how the data were collected via *Arduino*-program. It gave a better understanding of the test set-up so the following experiments using the same test set-up would work without difficulties.



# Appendix II - Lift and power experiment

This experiment was designed to test the power consumption of the motor compared to the lift that was created from the propeller. It was done with a BLDC motor and a fixed propeller namely a *GWS EP 7035* which is a propeller with a 190,5 mm diameter and a 114,3 mm pitch. The motor was fixed at different servo positions and the thrust and power consumption was measured.

## Test design

The test design was made with the motor attached at the end of the lever. This motor, with the propeller connected to it, was connected to an ESC (electronic speed controller). From the ESC the system was connected to the Arduino hardware and a power supply acting as the battery. A picture of the setup can be seen on figure 3

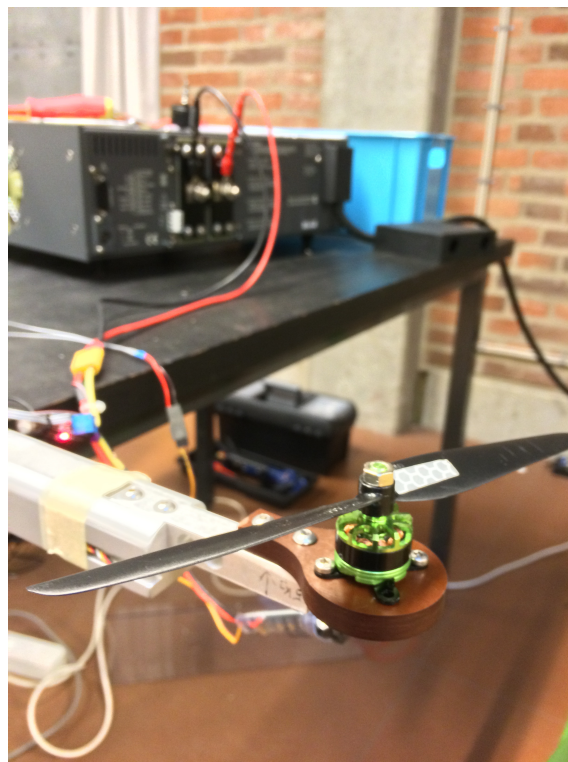


Figure 3: A picture of the motor and propeller used in the test.

## The motor

The motor used was a *Turnigy Multistar 1704-1900Kv* which is a brushless 12 pole outrunner motor. A 13,5 g motor with a max current of 4,5 amps and max voltage at 11 volts, with a Kv of 1900. This *Multistar* motor is specifically designed for multirotor use.

An overview of the used items in this experiment.

- Power supply
- Turnigy Multistar Outrunner motor
- Turnigy 3020 Outrunner motor
- GWS EP 7035 Propller
- Tachometer
- Stroboscope
- Arduinio hardware

## Approach

The experiment started with a certain servo position where the voltage, current, power consumption, thrust and thrust per watt were measured with the hardware *Arduino*. The angular velocity was also measured with a stroboscope and notated. The servo position was then changed and all the variables were measured again. This was done with an interval of 50 from servo position 1.100 to 1.750. The test was run two times on two separate dates, where the servo position started at position 1.100.

## Results and experiment discussion

For each servo position there were a multiple of measurements. The manually measured angular velocity, the number of the measurements were not the same. Therefore, an average value were calculated using the *Mean function* in *Matlab*. The mean results of the *Turnigy Multistar 1704-1900Kv* was the following.

Servopos.	Thrust(g)	RPM	g / Watt	Watt	Volt	Ampere
1.100	5,5592	2.833	3,5629	1,5603	10,8480	0,1401
1.150	13,8690	3.591	5,2431	2,6452	10,8409	0,2400
1.200	21,7612	4.224	5,8702	3,7071	10,8334	0,3400
1.250	33,2400	4.835	6,9357	4,7926	10,8261	0,4424
1.300	52,6011	5.507	7,5771	6,9421	10,8124	0,6419
1.350	65,5249	6.219	6,9009	9,4951	10,7813	0,8809
1.400	84,7641	6.847	6,8564	12,3628	10,7521	1,1497
1.450	103,7144	7.400	6,6072	15,6971	10,7213	1,4634
1.500	121,5744	7.927	6,4316	18,9025	10,6762	1,7703
1.550	143,6569	8.459	6,1272	23,4459	10,6619	2,1989
1.600	164,0488	9.024	5,7638	28,4618	10,6371	2,6757
1.650	180,6942	9.470	5,4900	32,9135	10,5356	3,1241
1.700	191,7831	9.790	5,0734	37,8015	10,5513	3,5826
1.750	222,8439	10.187	5,1254	43,4781	10,4023	4,1794

Table 1: Turnigy Multistar 1704-1900Kv motor with GWS EP 7035 propeller test 1.

Servopos.	Thrust(g)	RPM	g / Watt	Watt	Volt	Ampere
1.100	10,4529	2.868	6,5768	1,5894	10,8199	0,1500
1.150	19,6845	3.576	7,4792	2,6319	10,8064	0,2400
1.200	29,2761	4.202	7,9358	3,6891	10,7822	0,3400
1.250	41,9862	4.778	8,6480	4,8550	10,7528	0,4520
1.300	57,4523	5.451	8,4235	6,8205	10,6813	0,6407
1.350	73,9922	6.134	7,8811	9,3885	10,6448	0,8823
1.400	92,6073	6.733	7,6153	12,1606	10,5847	1,1490
1.450	108,8259	7.278	7,0833	15,3638	10,5631	1,4540
1.500	123,2617	7.780	6,6184	18,6241	10,4985	1,7737
1.550	141,6191	8.283	6,2575	22,6320	10,4384	2,1681
1.600	165,2178	8.774	6,1268	26,9662	10,3587	2,6031
1.650	181,6323	9.160	5,7920	31,3592	10,2886	3,0483
1.700	195,4931	9.569	5,4929	35,8513	10,1706	3,5252
1.750	215,0790	9.894	5,3379	40,2931	10,0332	4,0160

Table 2: Turnigy Multistar 1704-1900Kv motor with GWS EP 7035 propeller test 2.

As it can be seen on table 1 and 2, and by figure 4, the *Turnigy Multistar 1704-1900Kv* is most effective around 4.000-6.000 RPM, but since the quadcopter weighs about 400 grams, every one of the four motors would have to generate about 100 grams of lift. For this to happen, the quadcopter would have to operate around 7.000 RPM, where the thrust generated per watt is about  $7 \frac{g}{w}$  compared to the lower RPM, where the thrust per watt is  $7,5 \frac{g}{w}$ . The same phenomenon can be seen on figure 4, where an increase of  $\frac{g}{w}$  can be seen on the curve around 5.500 RPM.

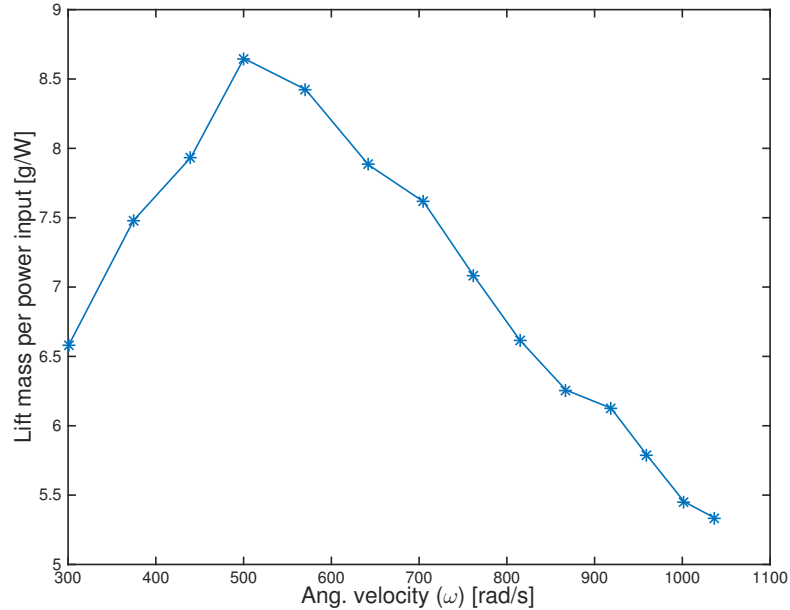


Figure 4: Gram per watt over RPM for the test with the Turnigy Multistar.

It is also possible to calculate the propeller constant in this experiment. This is done by

plotting the thrust over RPM and then drawing the best polynomial curve.

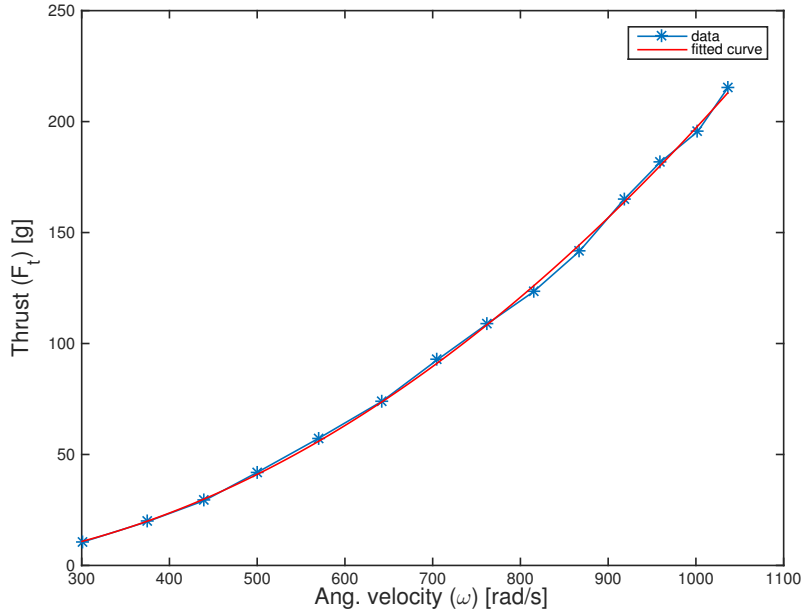


Figure 5: Finding the propeller constant for the test with the Turnigy Multistar

By figure 5, it can be seen that the propeller constant for this motor/propeller combination is  $2,6 \cdot 10^{-6} \cdot \omega^2 - 0,0057 \cdot \omega + 0,59$ . Theoretical the propeller constant should be equal to  $b\omega^2$ , the test results shows that there is an extra  $x\omega$  part which is due to losses in the system.

### Plausible deviations

There are some plausible deviations with the data, which could have occurred during the test. Since the test was done over two separate days temperature of which the motor could have been slightly different from each other. This could have lead to different outputs. Another thing that could have an effect on the results was that the first test was done with the light on where the second test was done with the lights off. A stroboscope is more precise in a dark environment and the results can have been affecting the results.

### Calibration errors

The lever was calibrated with the *Arduino* software/hardware before the first test, by turning the lever upside down and using it as a weighing scale. The calibration showed that the printed result from *Arduino* was 8 g too high, this was then subtracted from the result of the first test. Before the second test, the speed controller was taped on to the lever, hence it during the first test was hanging freely above the ground. Calibration showed that before the second test the results were only off by 2 g, which was substrated from the data sets, meaning that the position of the speed controller had an influence on the results.

# Appendix III - Mechanical losses - experiment

This experiment was designed to determine the different coefficient due to friction and drag, as described in *Mechanical losses*.

## Test design

The test design from *Appendix II - Lift and power experiment* is repeated with only one set of motor/propeller. The voltage drop across the motor at a given  $\omega$  to the time,  $t$ , is measured by an oscilloscope.

An overview of the used items in this experiment.

- Power supply
- Turnigy Multistar Outrunner motor
- GWS EP 7035 Propeller
- Differential probe
- Tachometer
- Oscilloscope
- Arduino hardware/software

The experiment is approached by measuring the CEMF when the motor is in cut-off mode, and due to the relation between the CEMF and the angular velocity, the characteristic of the angular velocity as a function of time can be found.

## Results

The CEMF is measured by connecting the oscilloscope to the terminals of the motor through a differential probe. The data is shown in figure 5.11.

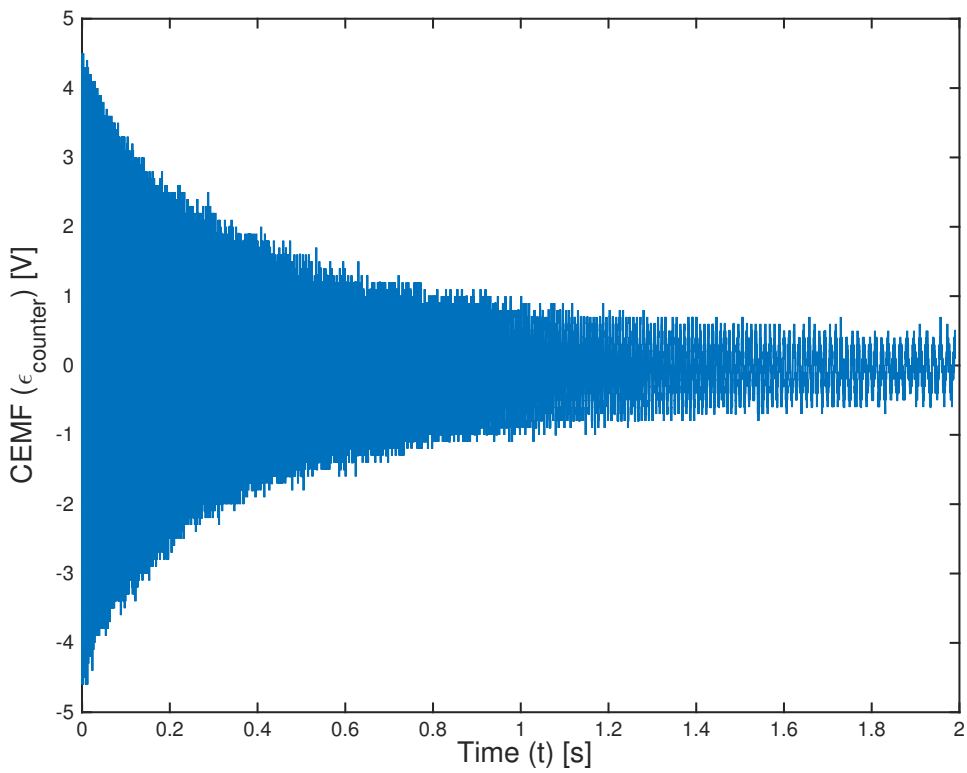


Figure 6: The graph shows a characteristic over the angular velocity as a function of time, when the motor the operation in cut-off mode.

### Plausible deviations

Since the purpose of the this experiment is to find the to determine the different coefficients due to friction and drag, and the measurements yield the induced EMF over a period of time. In order to get the desired results, the data set has to be analysed numerical, which is performed by plotting the data, and finding the best fitted curve. Since the data fluctuates around this curve, it is an approximation. Furthermore, numeric differentiation over the data set is performed, which is a method to estimate the behaviour of the curve. Since such numeric calculation is performed several times, it is reasonable to assume that the deviation increases.

# Appendix IV - Matlab scripts

## Hover time

To calculate the hover time for a quadcopter a Matlab script has been design. This script is loaded to a CD enclosed with the project report. By loading the experiment data into the script, such as thrust (in grams lift), rad/s, power and gram per watt, the script can calculate the hover time . When the data is loaded into the system, the given frame, motor, propeller and battery weight, battery voltage and battery capacity (in mAh) is set as constants or as input values. All weights are in kilogram. A part of the script, where some of the inputs are defined can be seen on figure below:

```
MM = input('If you want to write input data yourself write 1,'
'if you want our fixed values write 2:');
if (MM ==1)
%Input the different component values
n = input('enter the numbers of motors/propellers: ');
m_frame = input('enter value of the frames mass: ');
m_motor = input('enter value of the motors individual mass: ');
m_battery = input('enter value of the battery mass: ');
m_propeller = input('enter value of the propellers mass: ');
U_bat = input('enter value of the battery voltage: ');
Capacity = input('enter value of the battery mAh: ');
else
n=4;
%input mass
m_frame=0.09;
m_motor=0.0135;
m_battery=0.114;
m_propeller=0.005;
U_bat=7.4;
Capacity=2200;
end
```

The program at first finds the total mass of the system,  $m_{total}$  (the black box is set to a constant of 50g). Subsequently it calculates the weight that each motor has to lift to hover ( $m_{total}$  divided by four) and converts the kilograms to grams. This constant is called  $m_{liftg}$ , because it is the mass in gram each motor should lift. Hence, it calculates a fit for the Thrust over rad/s curve, where  $x_1$  is the value of rad/s that the thrust required to hover is equal to  $m_{liftg}$ . Then the gram per watt over rad/s can be fitted. Now the watt

per motor can be calculated, because  $x_1$  (the rad/s required to hover) can be inserted in the fit from before to find the gram per watt that the motor produces to lift the system, the gram per watt to the rad/s is called  $g_{wfor rpm}$ . Below is a part of the program where the fits is used:

```
%Each motor lifts a fourth of the weights
m_loft=m_total/n;
m_loftg=m_loft*1000;
%when the motor lifts with the mass in grams the quadcopter will hover.
% f2 is a fit that gives the thrust to rad/s
% the script calculates the rad/s called x1.
f2=fit(rads1,thrust1fixed,'poly2');
cf_coeff = coeffvalues(f2);
a = cf_coeff(1);
b = cf_coeff(2);
c = cf_coeff(3);
x1=(1/2)*(-b+sqrt(-4*a*c+4*a*m_loftg+b^2))/a;

%x1=(1/2)*(-b+sqrt(n*m_loftg*a-n*a*c+b^2))/a;
%f3 is also a fit, that gives a function to calculate lift gram per watt to
%a specific rad/s.
f3=fit(rads1,g_wfixed,'poly2');
cf_coeff = coeffvalues(f3);
d = cf_coeff(1);
e = cf_coeff(2);
u = cf_coeff(3);
g_wfor rpm=d*x1^2+e*x1+u;
```

When the gram per watt, the quadcopter requires to hover, is known and the weight of each motor, the watt per motor can be calculated as  $wattpermotor = m_{loftg}/g_{wfor rpm}$ . The total watt,  $Watttotal$ , is then  $wattpermotor$  times four motors, called  $watttotal$ . Thus the hover time can be calculated by knowing the battery voltage  $U_{bat}$  times the capacity  $C$  (in ampere seconds). Then by dividing this result by  $watttotal$  the hover time in seconds is calculated. The function  $hms$  converts the hover time in the program to hours, minutes and seconds. An example of the functions and relations, which the program gives is shown in section *Hover time*. The part of the program, which plots the graphs and shows the final results:

```

%Plots rad/s on the x axis and grams per watt on y axis
subplot(1,2,2) % second subplot
plot(rads1,g_wfixed)
hold on
f2=fit(rads1,g_wfixed,'poly2');
plot(f2,rads1,g_wfixed)
hold on
hx = graph2d.constantline(x1, 'LineStyle','-', 'Color',[0 1 0]);
changedependvar(hx,'x');
hy = graph2d.constantline(g_wforrpm, 'Color',[0 1 0]);
changedependvar(hy,'y');
xlabel('Ang. velocity (\omega) [rad/s]')
ylabel('Gram per watt [g/W]')
else
    hold off
close all
end
%Results: |hovertime| |g/w/rpm| |w/motor| |RPM| |totalmass| |gram per watt
results = [hovertime g_wforrpm wattpmotor x1 m_total g_wforrpm]
%Hovertime in hours minutes seconds:
hms

```

## Electromechanical torque and efficiency

The second part of the script calculates the motor torque and efficiency of the motor. The test data used in this part is found in an motor expiration experiment where the motor is cut off and the time and EMF are measured. The data is loaded and since a oscilloscope is used to measure sinus waves 10.000 data is imported. In order to find the angular acceleration every wave peak point has to be found and every negative value eliminated. The time has to match in dimension in order to be able to plot it, therefore all time variables that does not correspond with the peak values are removed. Now the motor constant  $K_\varphi$  can be found with the measured angular velocity just before the motor is cut off. This can be seen on the figure just below:

```

%Regulates the time due to lab data displacement
tid3=tid2+1.01;
U2=U2+1.2;
%eliminates all negative values
U3=U2(tid3<=2);
U4=U3(U3<=0);
U4=U4*(-1);
%finds local maxima
peaks = findpeaks(U4);

%macthes variables to have same dimensions
tid4=tid3(peaks==peaks);

%plots time over peak voltages with a power regression
F=fit(tid4,peaks,'power2');

% The angular velocity
k = 4.6/(9450*(2*3.1415/60)); %Variates with the motor.
%E_1 = input('Enter value of E_1: ')
%k = E_1 / w_1;
w = (peaks./k);
```

The angular velocity over the time is plotted and a fit for the regression is found. This is done to find the angular acceleration in relation to the time. This formula is then differentiated with relation to time to find the angular acceleration. The torque due to the moment of inertia is given by the angular acceleration multiplied by the propeller's moment of inertia. To find this, the angular acceleration are found for each time variable. This can be seen on the figure below.

```

F2=fit(tid4, w, 'power2');
%Finding the constants a, b, c. for power regresion 2
cf_coeff2 = coeffvalues(F2);
a1 = cf_coeff2(1);
b1 = cf_coeff2(2);
c1 = cf_coeff2(3);

%Differentiates the forumla from F2 to get the angular acceleration
%the double matlabfunction converts functions to variables

syms f(x)
%formula for power regression
f(x) = a1*x^b1+c1;
syms g(x)
%f(x) differentiated
g(x) = diff(f(x));
%the differentiated formula with respect to the time
g_t=double(g(tid4));

%Inertia
J = -7.29769 *10^-7; %input('input value of J: ');

% t_J equals the inertia torque
t_J = g_t.*J;
```

The torque due to the moment of inertia is then plotted over the angular velocity with a polynomial regression. The constants of the best fit are now the power losses of the system and the electro mechanical torque can now be found using these constants. The efficiency is now  $\frac{P_{out}}{P_{in}} \cdot 100$  where  $P_{out}$  is calculated from the the torque multiplied

by the angular velocity, and  $P_{in}$  is the measured power from the first test. This can also be seen on the figure below:

```
%the torque can now be found
torque=p1.*rads.^2 + p2.*rads + p3 + t_J;

%watt = torque * rad/s
Pem=torque.*rads;
|
%ha is the equation for Pout as a function of radians per second.
%ha=formula(F5);
syms ha(x)
ha(x)=q1*x^q2;
wattcalculated=double(ha(rads2));

efficiency=wattcalculated./watt2;
efficiencypercent=efficiency(efficiency<=1);
rpmeff=rads2(efficiencypercent==efficiencypercent);

Pout=double(ha(x1));
effe=(Pout/wattpmotor)*100;
```

At the end the program plots the motors efficiency over the angular velocity.



# Appendix V - Modification of the discharge time equation

The relation between discharge time and discharge rate is described by *Peukert's law* [D. Baert, 1999]. This is a more accurate method to determine the discharge time of the battery, because it factors in more variables regarding the quantities and qualities of the battery. The reason this method is not considered in the project is due to the fact that these variables are not given by the manufacturers and are difficult to find experimental.

## Peukert's Law

The capacity of the battery refers to the amount of electrical charge it is able to deliver at the rated voltage. *Peukert's Law*, outlined in equation 4, expresses the time of discharge,  $t_d$ , under a particular load, which can be described as the current drawn from the battery,  $I$ .

$$t_d = H \left( \frac{C}{I \cdot H} \right)^k \quad (4)$$

Here  $H$  is the rated time the battery can discharge measured in hours.  $C$  is the capacity at a the rated discharge time,  $k$ , is Peukert's constant, and  $I$  is the current drawn from the battery. From equation 4 it appears that the time of discharge and the current - to power of  $k$  - drawn from the battery are inverse proportional. Hence, the greater current drawn, the shorter time of discharge. The discharge time is related to the hover time of the quadcopter. This correspond to letting  $k$  equal one in equation 4.7.